

Chapter 7 Accelerator Structures III - RFQ

SNS Front End

RFQ Basics I – Transverse Focusing

RFQ Basics II – Beam Dynamics

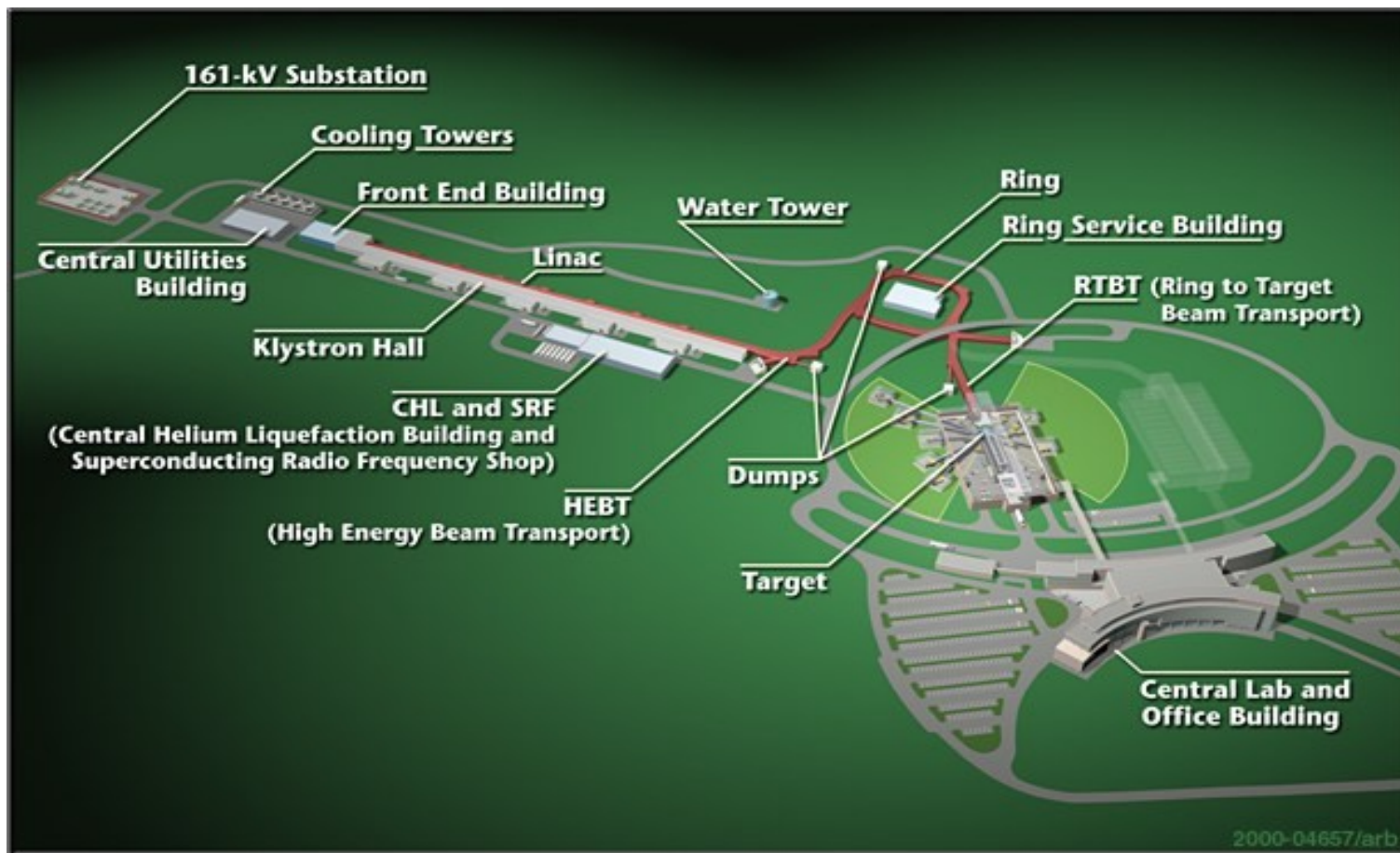
Structure Calculation with Superfish

Parmteq, Curli, RFQuick

Appendix: beam dynamics details

Design Example, the SNS RFQ

The Spallation Neutron Source, located at the Oak Ridge National Laboratory, is the USA's newest large-scale acceleration project. Now (2007) undergoing commissioning, it will be the world's most powerful pulsed neutron source, providing a 1 GeV proton beam with average power of 1.4 Megawatts to a liquid mercury target. Currently being tested at the 100 kW level (March 2007), it will achieve full-power operation in 2008-09.



SNS RFQ Requirements

The overall SNS systems optimization resulted in the requirements for the RFQ subsystem.

Frequency	402.5	MHz
Output Energy	2.5	MeV
Pulse Length	1.0	msec
Pulse Current	38	mA
Pulse Rate	60	Hz
Transverse Emittance	0.27	π mm-mrad

The other parameters were left up to the designer of the RFQ itself. These parameters include

Injection Energy
Vane Voltage
Aperture

and many other mechanical, electrical and beam dynamics parameters. An optimization was undertaken to maximize performance and reliability at minimum cost.

The SNS Linac

The SNS linac delivers a 38 mA H⁻ beam pulse, 1 msec in duration, at a 60 Hz rate. The H⁻ beam is stripped to H⁺ during injection into a storage ring, where it is extracted in one turn, delivering a proton beam current of several amperes.

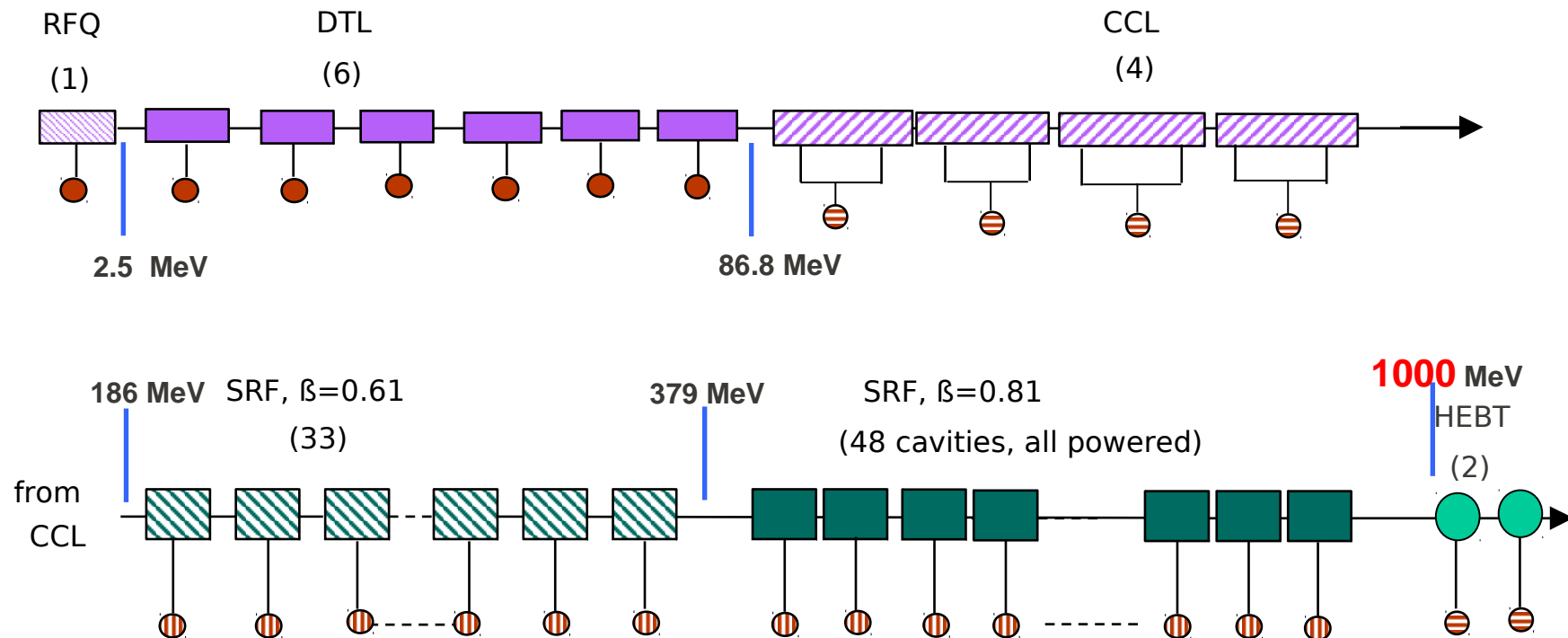
The linac is divided into four sections:

2.5 MeV RFQ

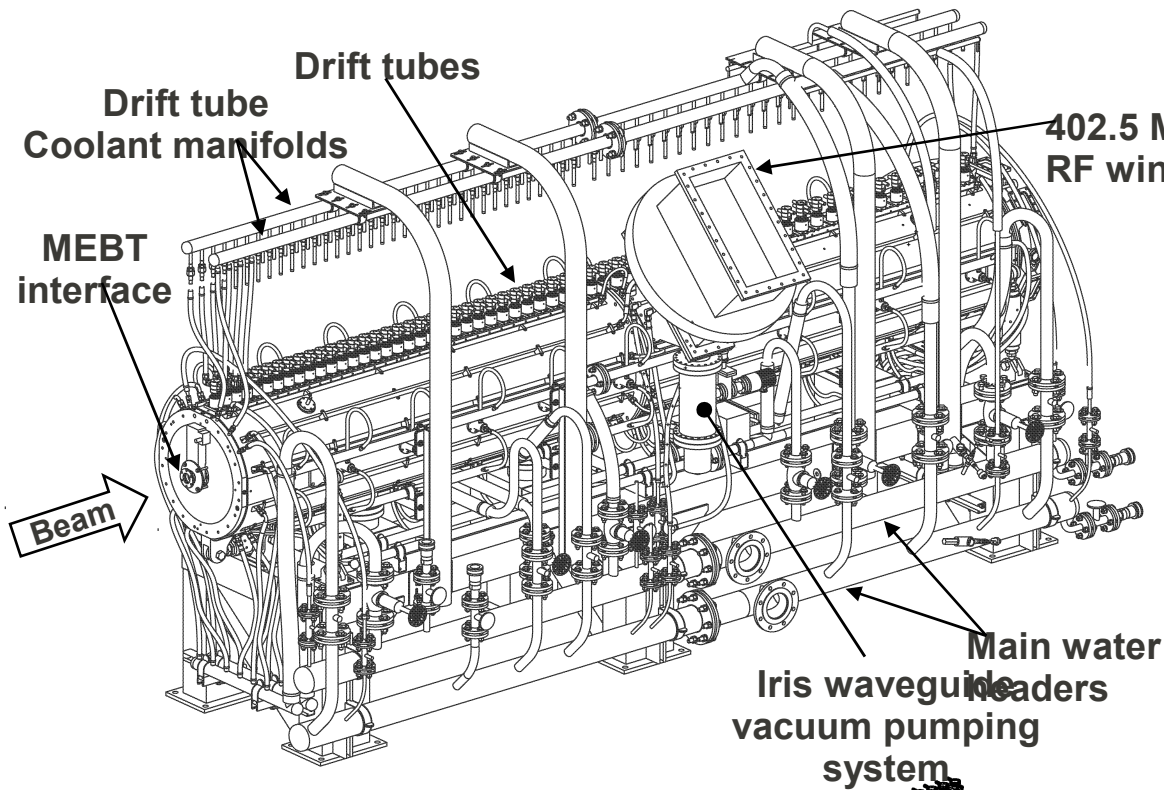
86 MeV Drift-Tube Linac

186 MeV Side-Coupled Linac

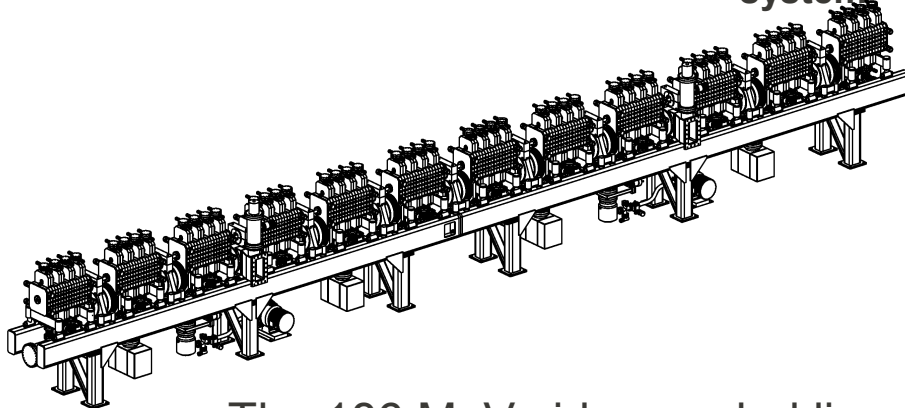
1 GeV Superconducting Linac, to be extended



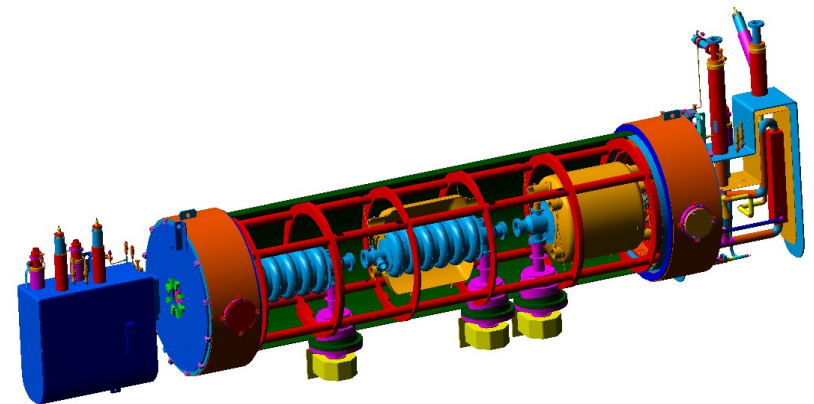
The Various SNS Linac Sections



The 402.5 MHz drift-tube linac.



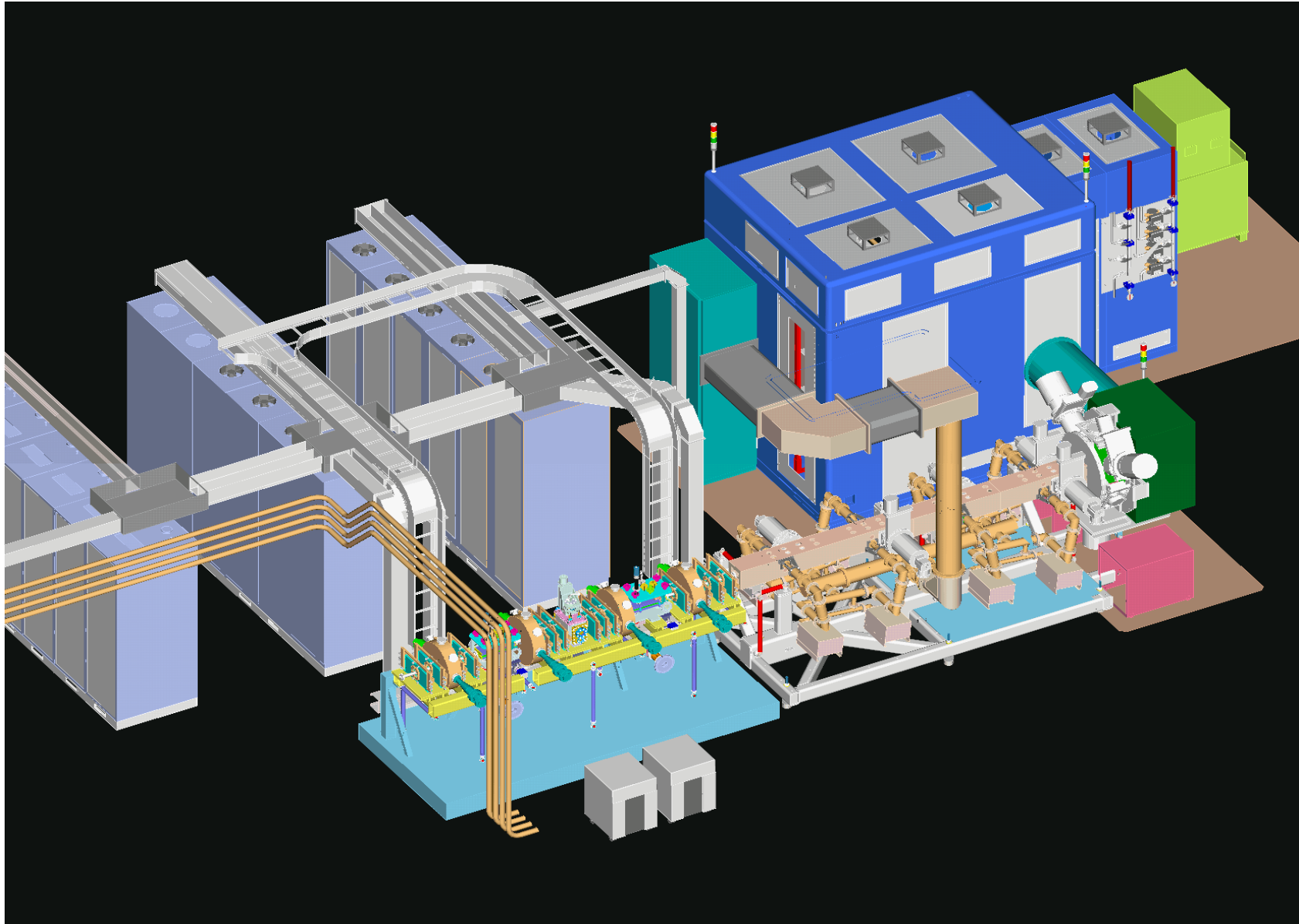
The 186 MeV side-coupled linac



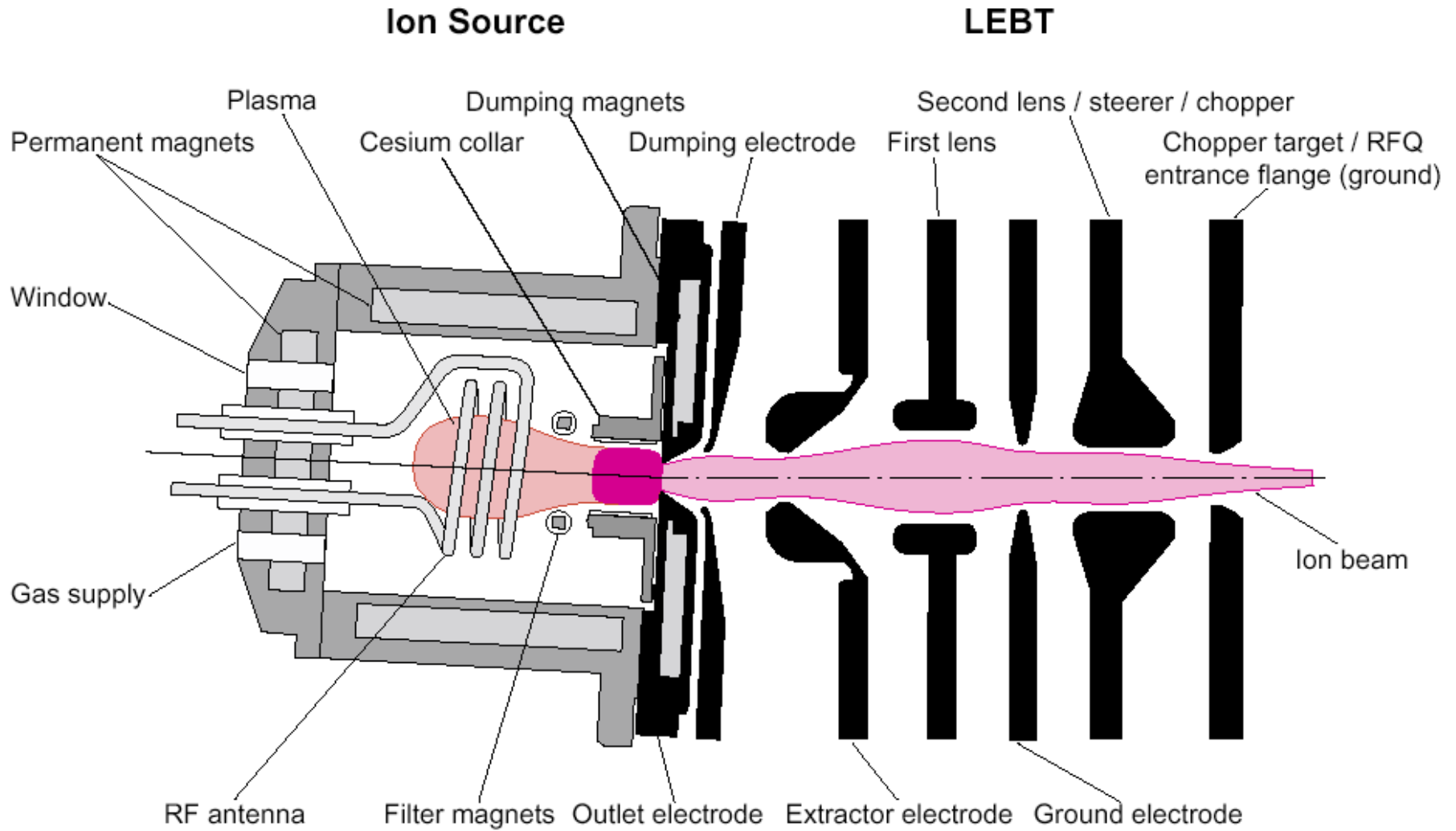
One cryostat of the 1 GeV superconducting linac

The Ion Source and RFQ

The ion source provides a 65 keV H⁻ beam to the RFQ.

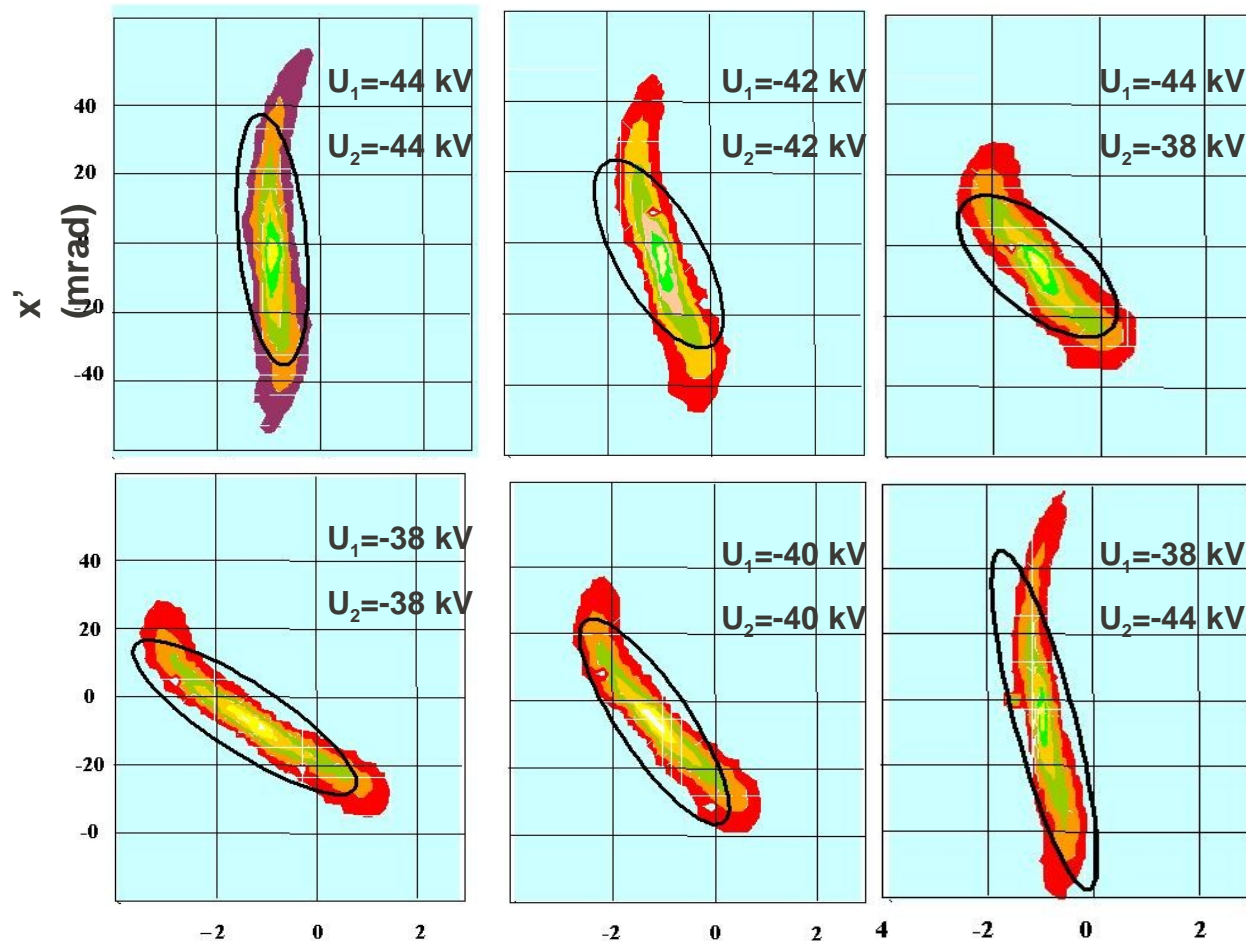


The H- Ion Source and Electrostatic LEBT

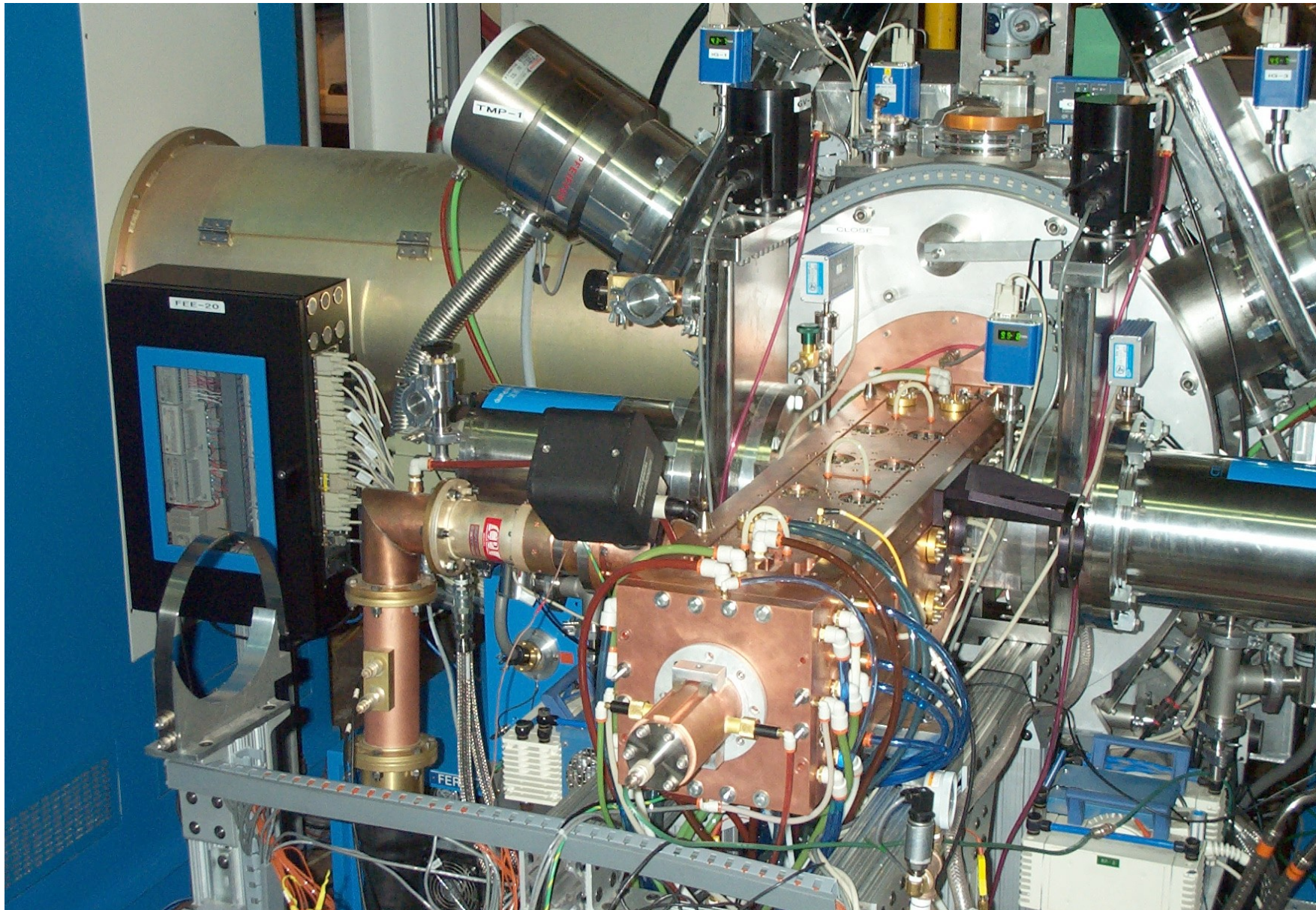


Simulation and Measurement of the Ion Source Phase Space

The simulation of the ion source and LEBT output beam with the PBGUNS codes is compared with the measurements at various lens voltages in the LEBT. The measured beam is compared with the simulated phase space ellipse (in black). This shows the expected accuracy of ion source simulations for H⁻ sources.

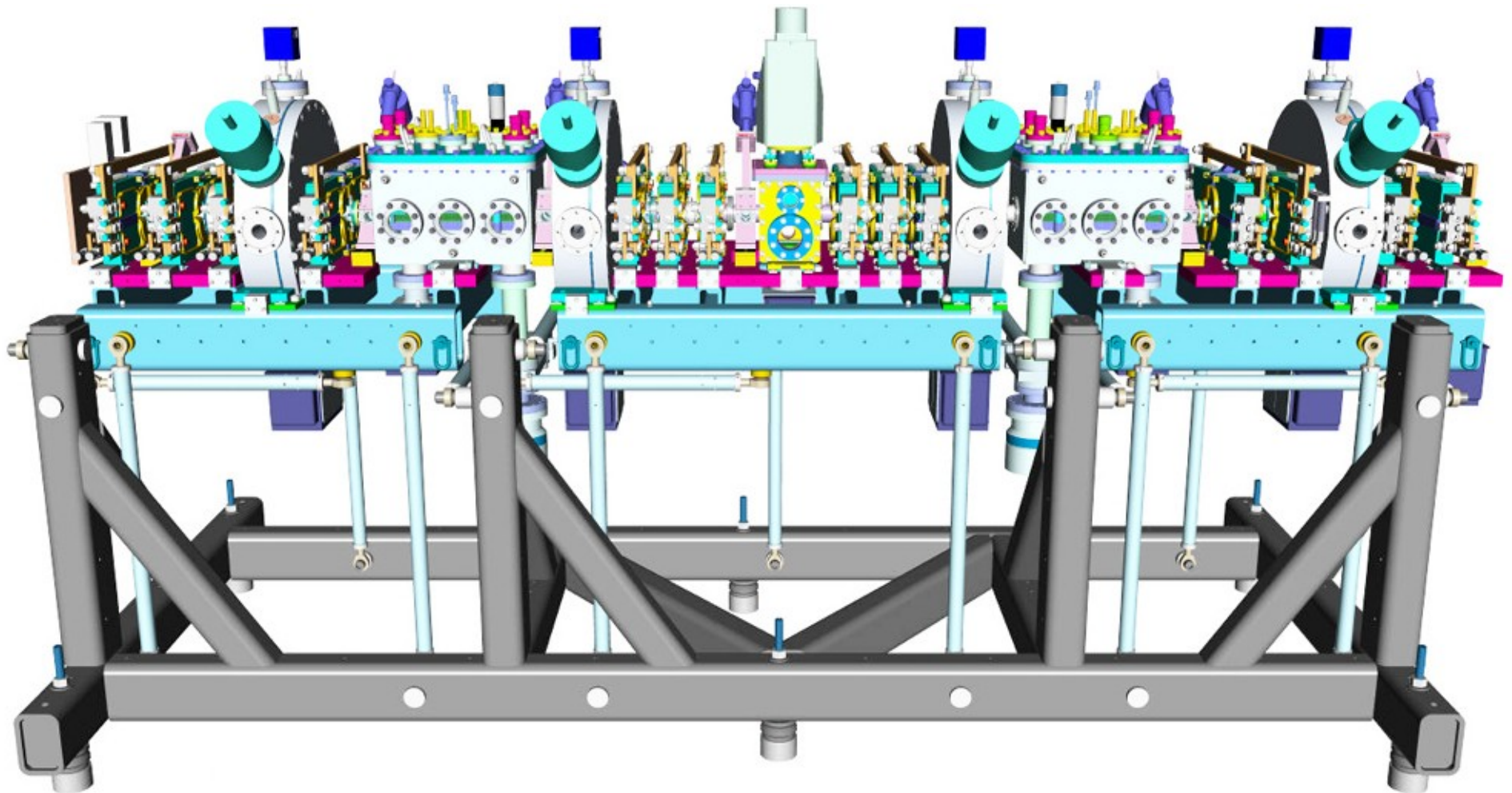


First Section of RFQ Mounted on Ion Source Chamber

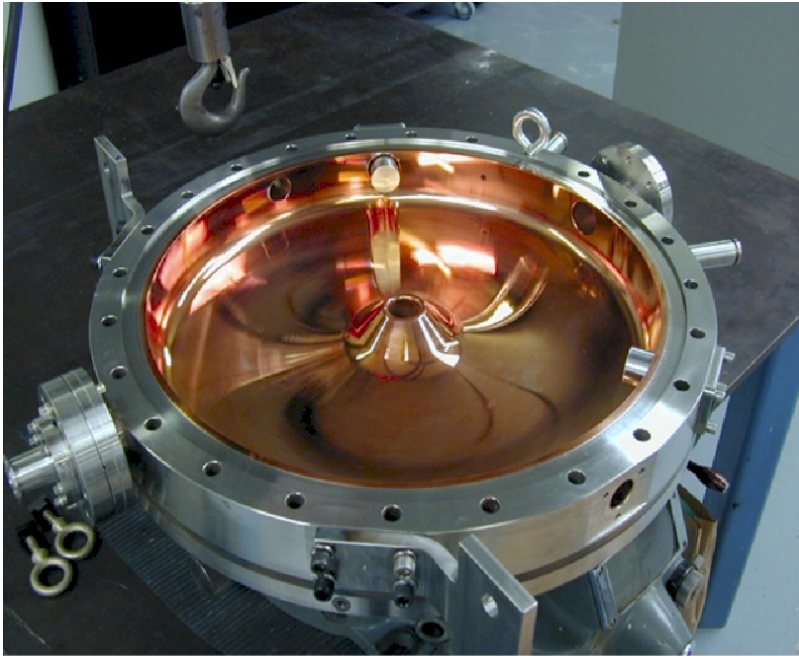


Medium-Energy Beam Transport System

The MEBT, following the 2.5 MeV RFQ, includes a beam chopper, 12 quadrupoles to focus the beam transversely and match it to the DTL input requirement, and 4 rebuncher cavities to focus the beam longitudinally.

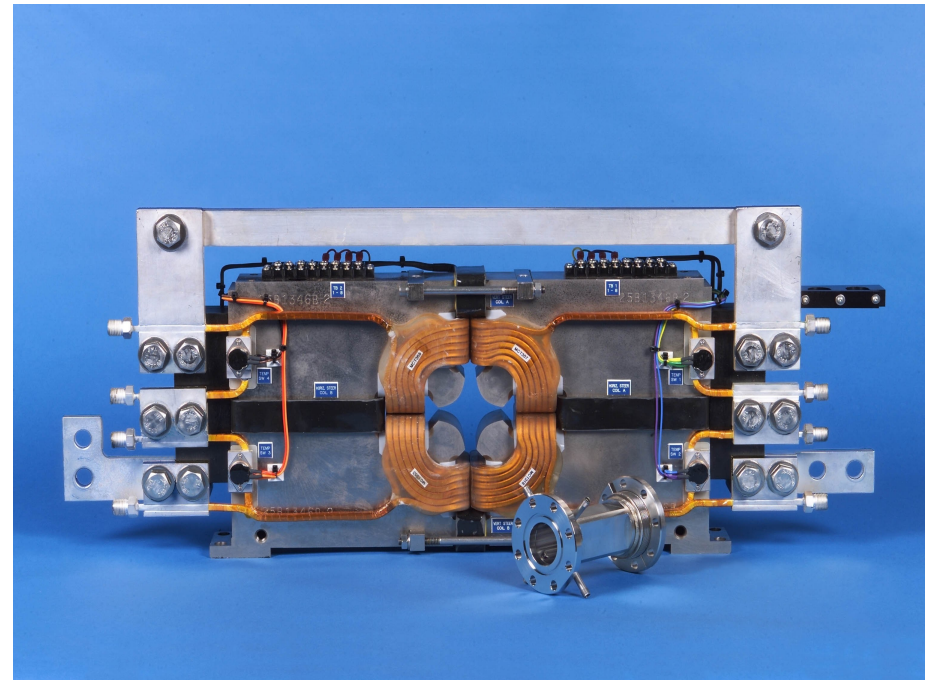


Some MEBT Components



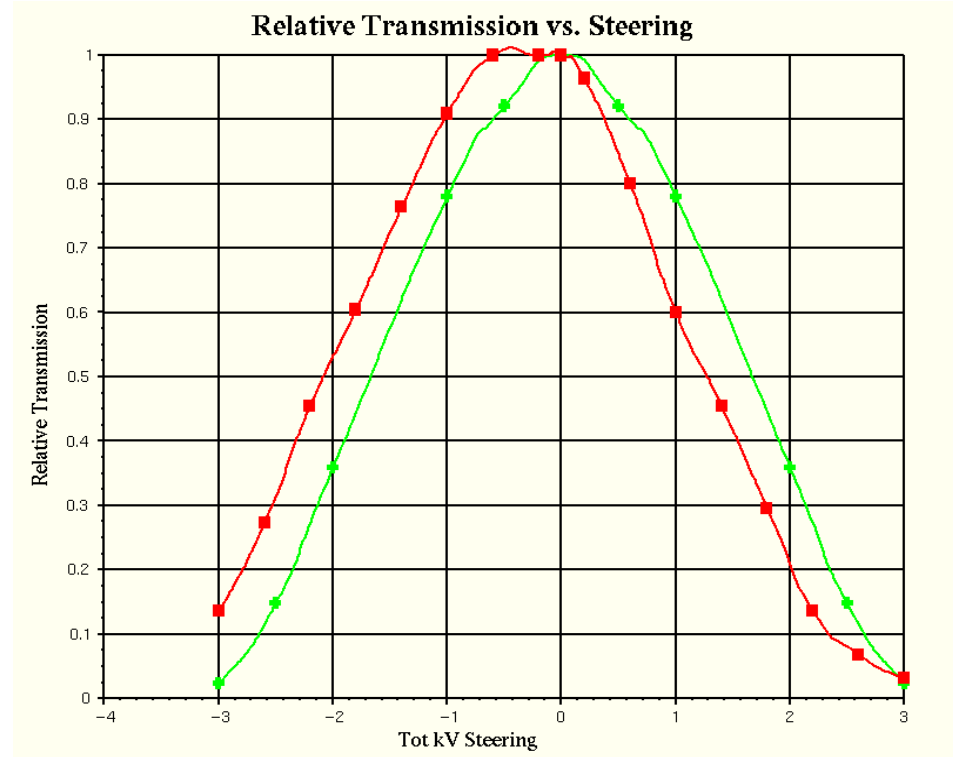
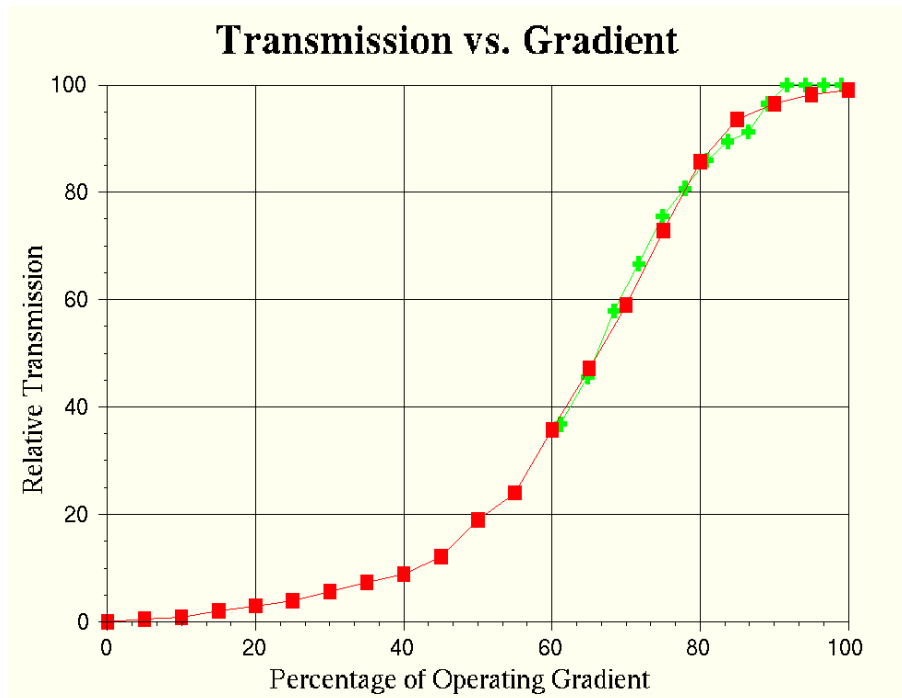
The interior of the pillbox rebuncher cavity (one-half shown) operates in the TM_{010} mode at 402.5 MHz. The gap voltage is about 65 kV.

Twelve quadrupoles provide transverse focusing. In the jaws of several of the quadrupoles is a beam position monitor (in front of the quadrupole) that provides beam position, intensity and timing information.



Agreement of Simulations and Measurements of the RFQ Transmission

The beam transmission through the RFQ is calculated with PARMTEQ as a function of the voltage on the vanes. The measured values (green) are in good agreement with the calculated values (red).



Many other parameters may be calculated, such as the transmission as a function of transverse offset of the beam at the entrance of the RFQ. Here, the measured transmission shows excellent agreement, but with a steering offset error.

RFQs

The RFQ is a low-velocity, high-current linear accelerator with high capture efficiency that can accelerate ion species from protons through uranium. Ion sources need only to operate at relatively low extraction voltage and pre-acceleration voltages to inject the RFQ.

The RFQ output energy is well matched to the input energy requirement of linear accelerators such as drift-tube linacs.



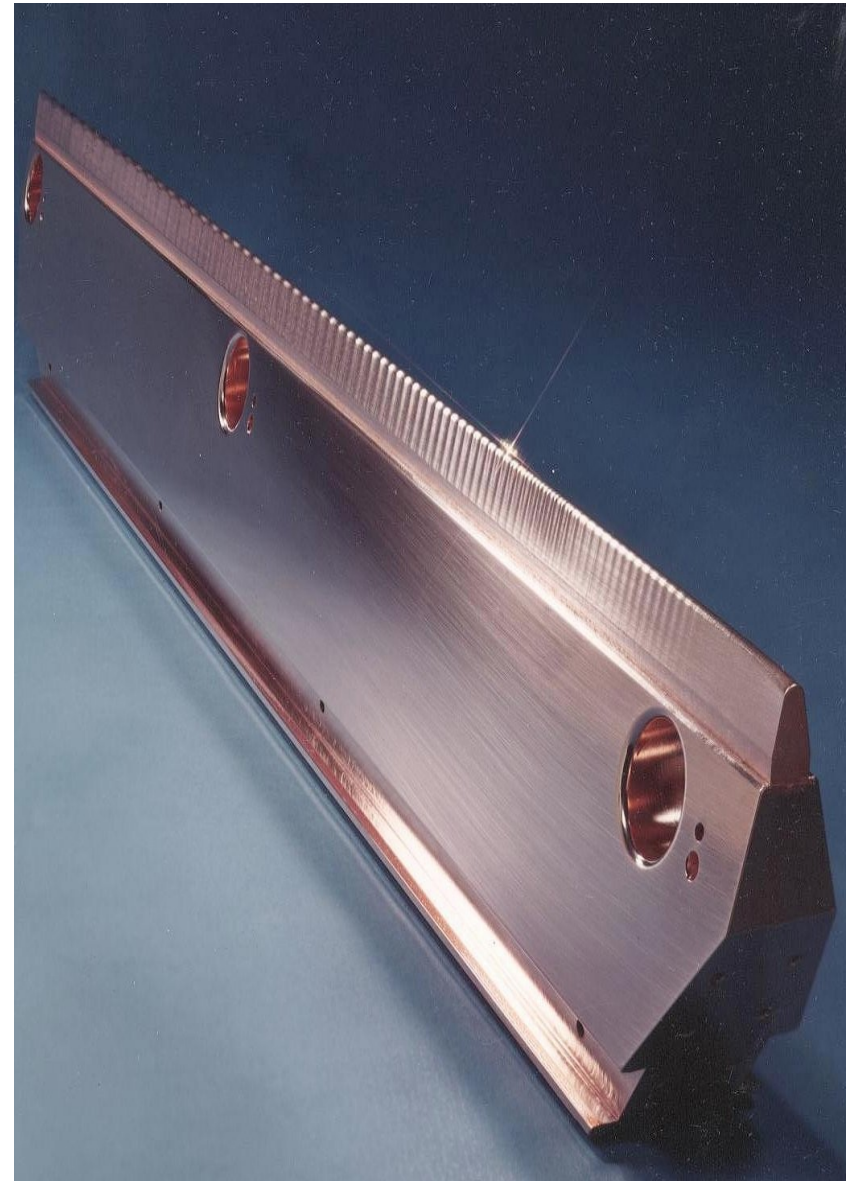
Many laboratories have adopted the RFQ as a front end accelerator for injectors for synchrotrons. The RFQ has almost completely replaced large 750 kV air-insulated Cockcroft-Walton accelerators (except at FNAL and LANSCE). RFQs have a smaller footprint and a lower cost of maintenance than CW pre-accelerators.

RFQ Characteristics

The RFQ is a unique kind of accelerator. It is fundamentally an alternating-gradient focusing channel, with acceleration added as a perturbation. In all other accelerator types, the focusing is added as a perturbation to the structure.

The accelerating field profile of an RFQ can be tailored to produce any functional form along the axis. This permits optimizing the accelerating field profile for high acceptance of the beam from the ion source, or optimizing other parameters such as the exit beam emittance.

The longitudinal field profile is almost independent of the transverse quadrupole focusing field and is established by the **modulations** along the vane tip.

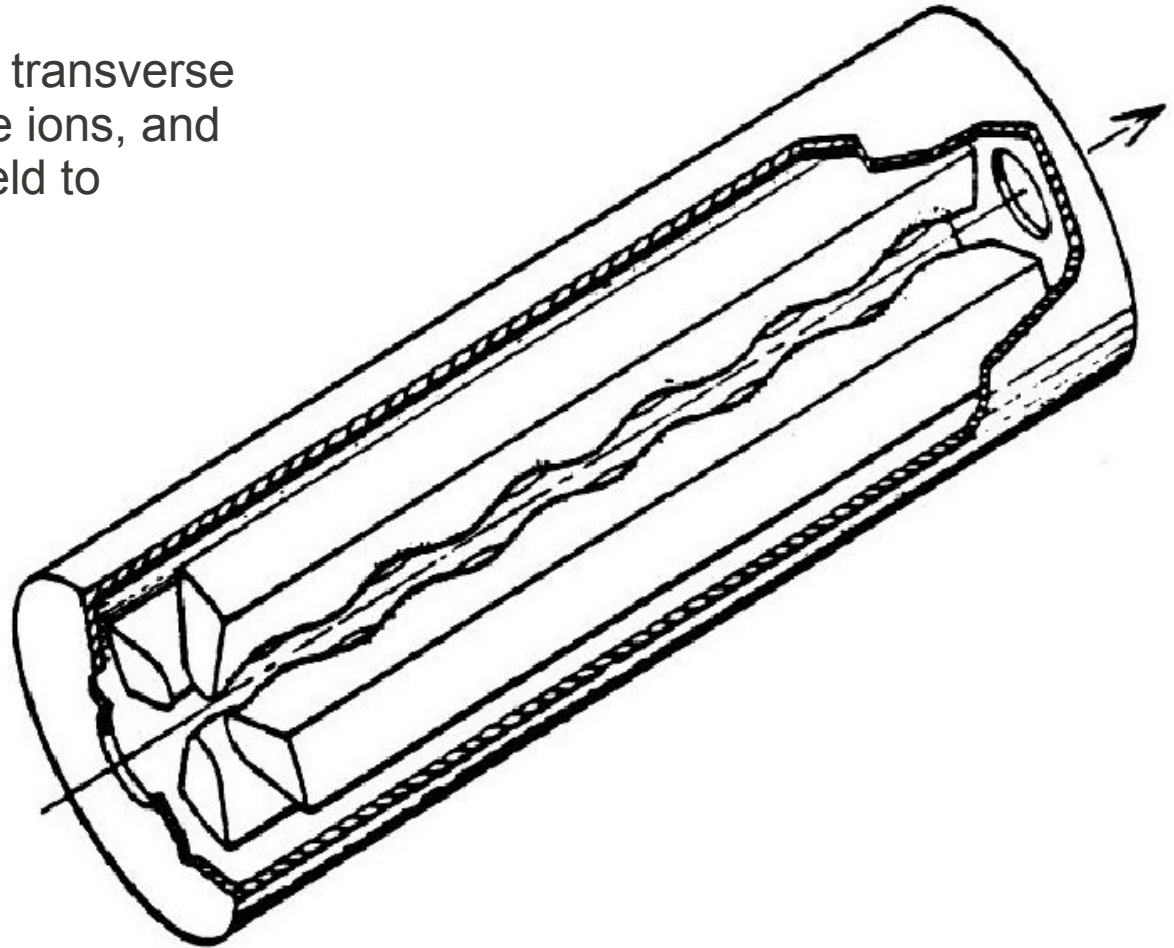


Principle of Operation

The RFQ accelerator uses a transverse electrostatic field to focus the ions, and a longitudinal electrostatic field to accelerate the ions.

The transverse alternating-gradient focusing results from the changing polarity of the RF field as the ion travels down the axis.

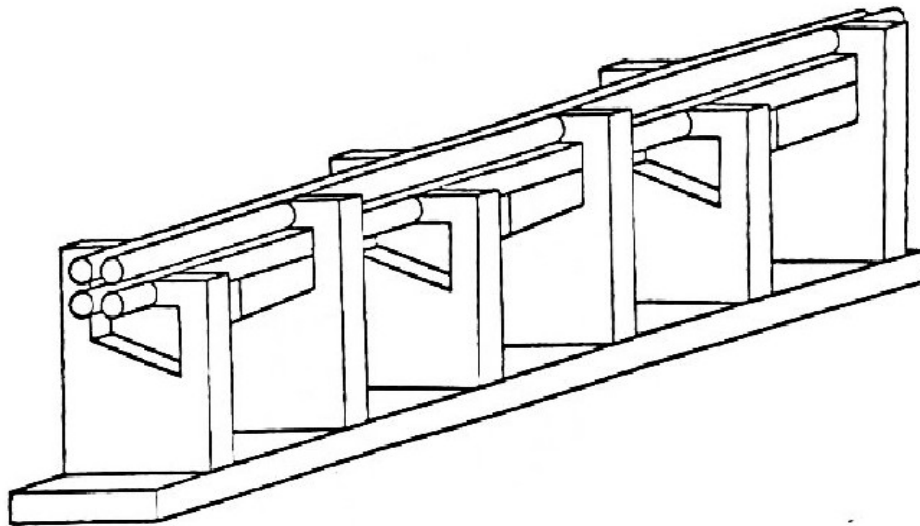
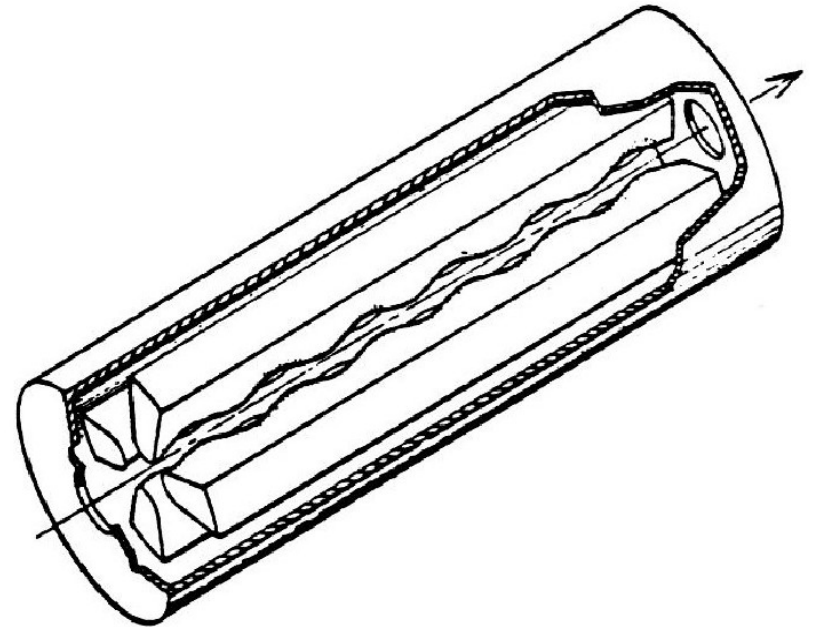
The ripples on the vane tip generate a longitudinal accelerating field and have only a small effect on the transverse focusing field.



RFQ Types

Most RFQs can be classified as one of two types: 4-vane and 4-rod RFQs.

The 4-vane RFQ is 4-fold symmetric and is generally used at frequencies from 200 MHz on up. This RFQ is subject to unwanted dipole modes, which can be eliminated with various additional components.



The 4-rod RFQ is generally used at frequencies of 200 MHz on down. It is non-symmetric, requiring more attention to thermal expansion issues, but has a simpler mode structure.

We will concentrate on the 4-vane structure in this course.

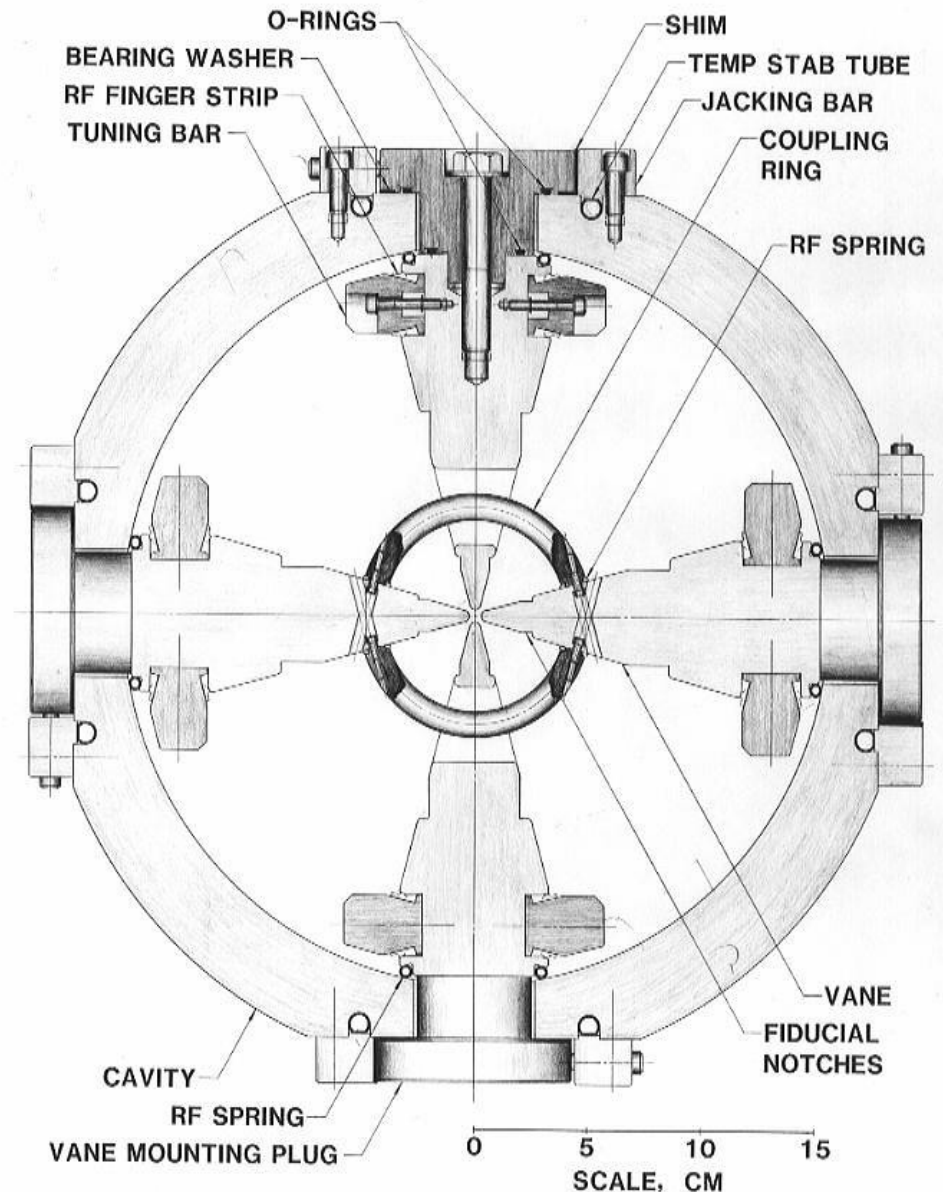
Components of a 4-vane RFQ

The RFQ consists of an outer **cavity wall**, comprising the vacuum chamber.

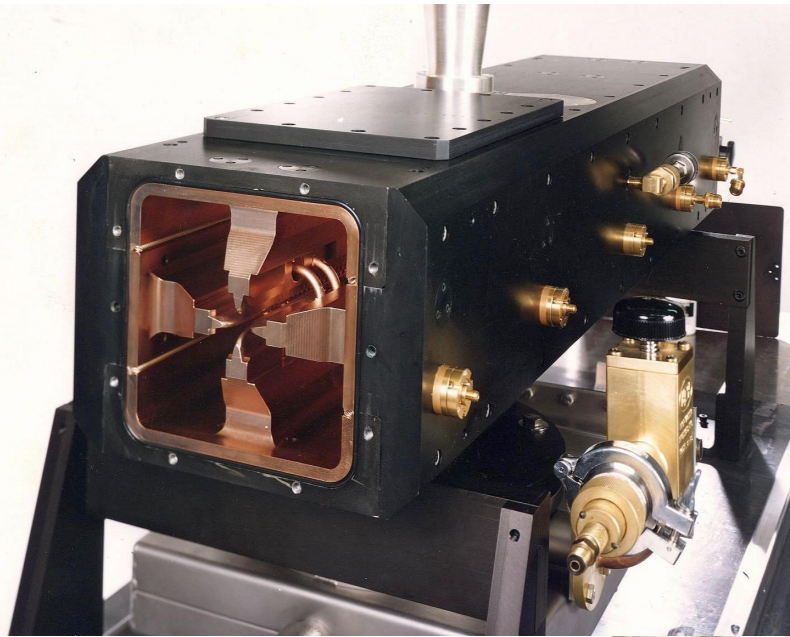
Within the cavity wall are **4 vanes**, arranged symmetrically. A TE_{210} quadrupole electric field is excited on the vanes.

The tips of the vanes have ripples, or **modulations**, that convert part of the TE_{210} field to an accelerating longitudinal field.

The RFQ cavity also includes a **tuner**, optional **tuning bars**, an RF **drive loop** and **vacuum ports**.



Wide Variety of Sizes



RFQs come in a wide variety of sizes, from a 1-meter long 0.8 MeV proton RFQ to a monster 6.9 MeV proton RFQ, both operating in the 400 MHz range.

The large RFQ is LEDA at LANL, which accelerates a 100 mA CW beam of protons.

It is shown buried in its cooling piping.

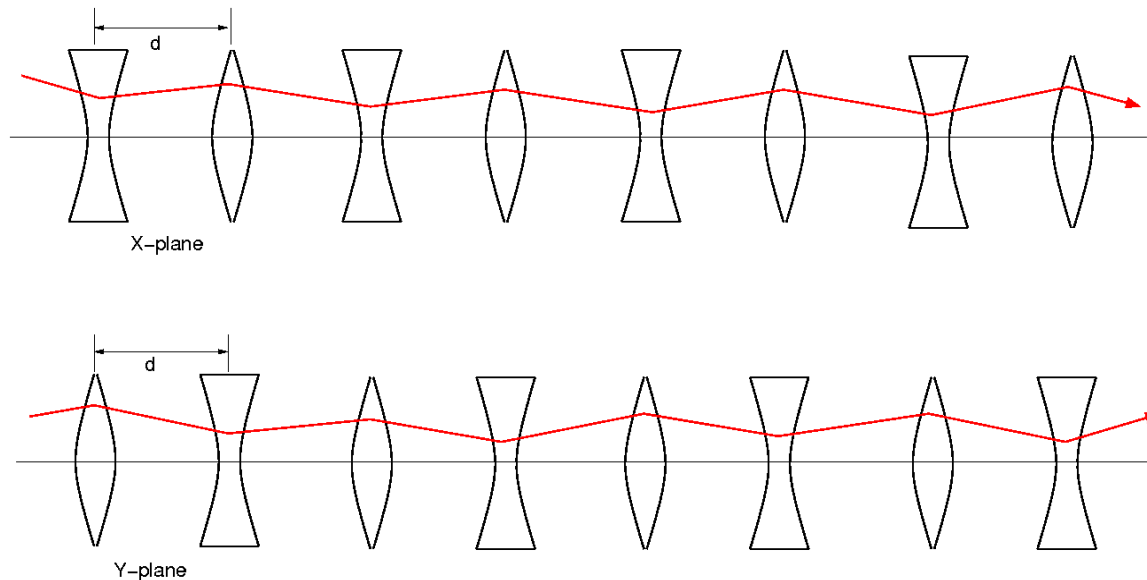
The small RFQ uses no cooling at all.



FODO Lattice

The RFQ is a unique type of accelerator that starts with a focusing lattice and adds acceleration as a perturbation.

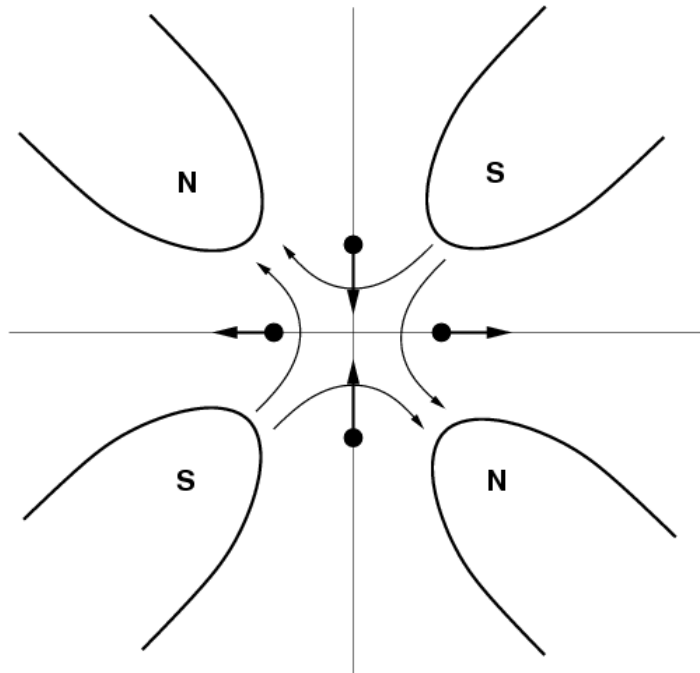
Recall that a sequence of focusing and defocusing lenses forms a **strong-focusing lattice**.



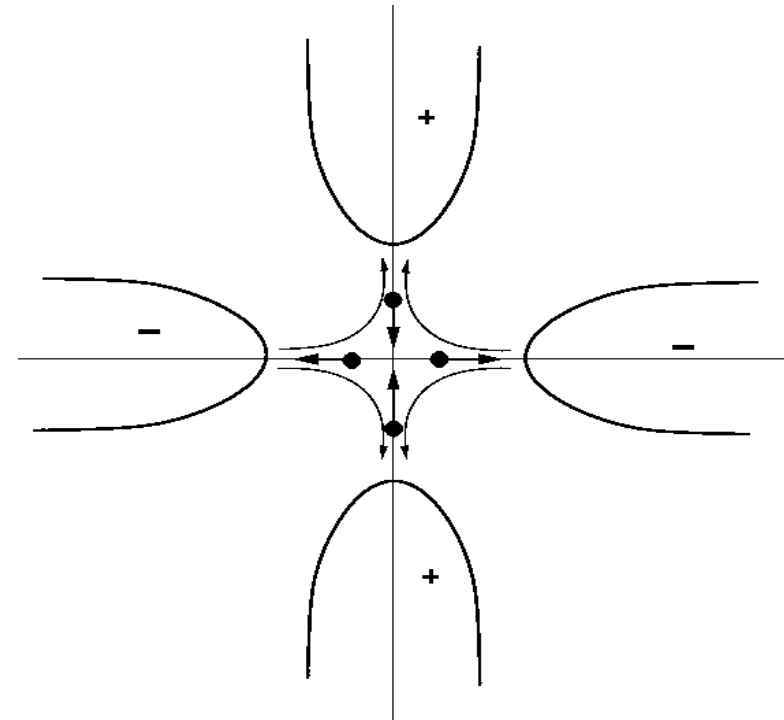
For certain values of the focusing/defocusing strengths and the distance between elements, a stable transport solution exists.

In addition, a **matched solution** exists that repeats the envelope for each period.

Magnetic and Electrostatic Quadrupoles



Vertically Focusing Magnetic Quad



Vertically Focusing Electric Quad

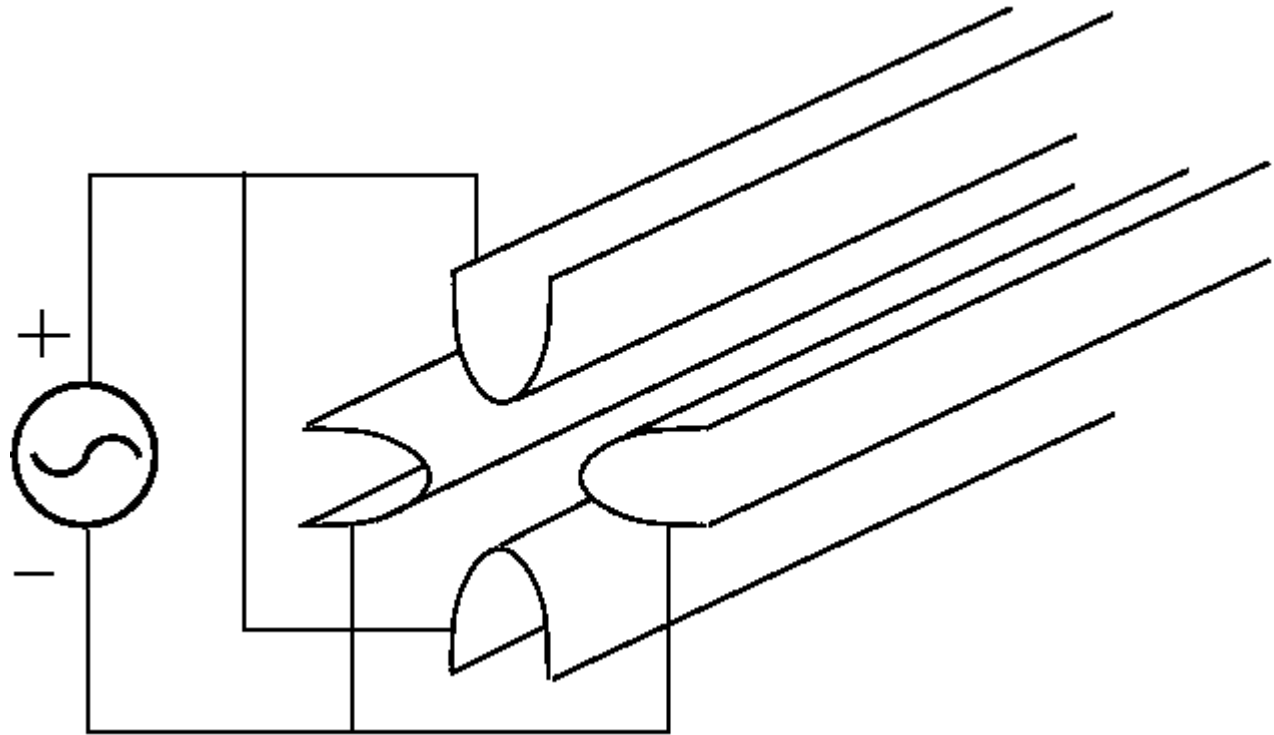
Note that the ES quad is rotated 45 degrees from the magnetic quad

A sequence of ES quadrupoles will form a strong-focusing sequence.

Alternating-Voltage Electric Quadrupole

An extended ES quad is powered by an alternating voltage source of frequency f or period $t = 1 / f$.

A positive ion of velocity $v = \beta c$ moves along the channel inside the quad.



The quadrupole field along the axis will vary as $\cos(\omega t)$, $\omega = 2\pi f$

As an ion moves along the ES quadrupole with velocity $v = \beta c$, it will experience an alternating quadrupole gradient.

The focusing is continuous, not discrete as with actual physical quadrupoles.

The alternating voltage on the ESQ is

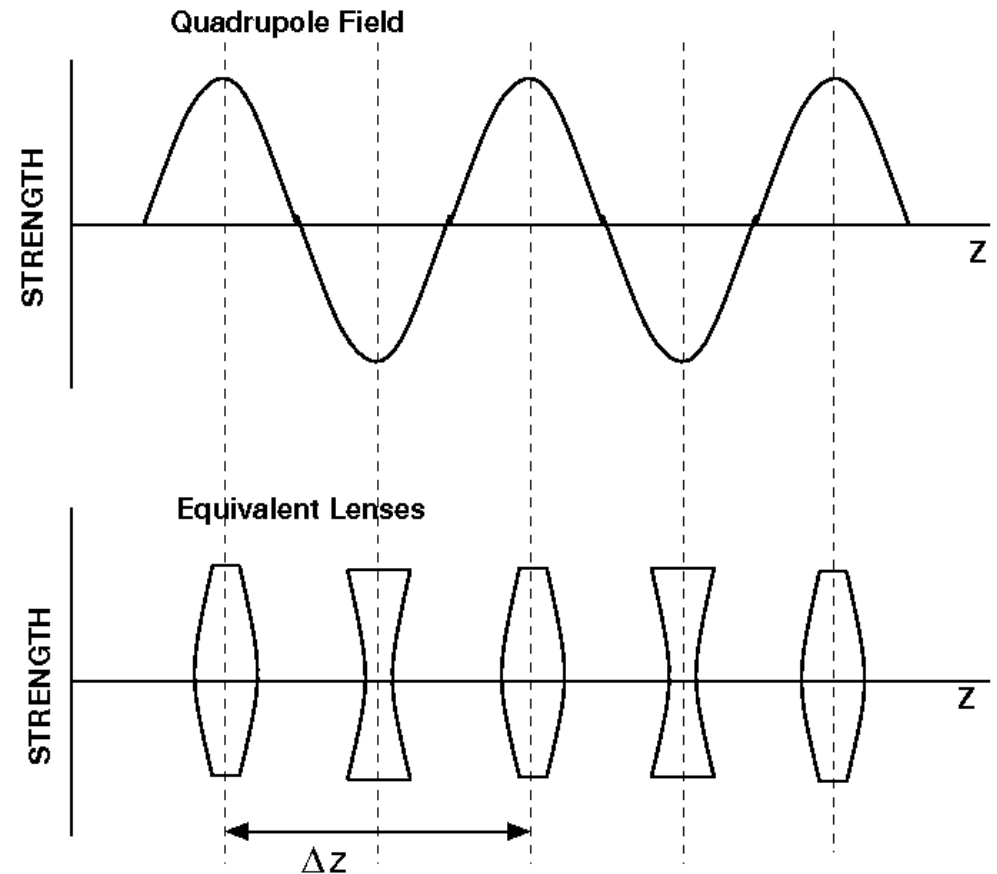
$$V(t) = V_0 \sin(\omega t)$$

The wavelength of the exciting frequency is

$$\lambda = \frac{c}{f}$$

And in one RF period, the ion travels

$$\Delta z = \beta c \Delta t = \frac{\beta c}{f} = \beta \lambda$$



The alternating field electrostatic quadrupole acts like a strong focusing sequence.

Transverse Equation of Motion for a Single Ray

Let $k = \frac{2\pi}{\beta\lambda} = \frac{2\pi}{L}$ kz advances by 2π as z advances one RF period

Equation of motion:
$$m \frac{d^2 x}{dz^2} = q e E_x = q e \frac{V}{a^2} \sin(\omega t) x$$

Let $B_0 = \left(\frac{q e V}{m c^2} \right) \left(\frac{\lambda^2}{a^2} \right)$, $\omega t \rightarrow k z$ a is the distance from the axis to the pole tip, V is the peak voltage.

And the equation of motion becomes **Mathieu's equation**, where an additional defocusing parameter has been added.

$$\beta^2 \lambda^2 \frac{d^2 x}{dz^2} = (B_0 \sin(kz) + \Delta) x$$

Which has two parts as the solution $x(z) = X(z) \sqrt{\beta(z)}$

Where $X(z)$ is a slowly varying function and $\beta(z)$ varies with the periodicity of the quads.

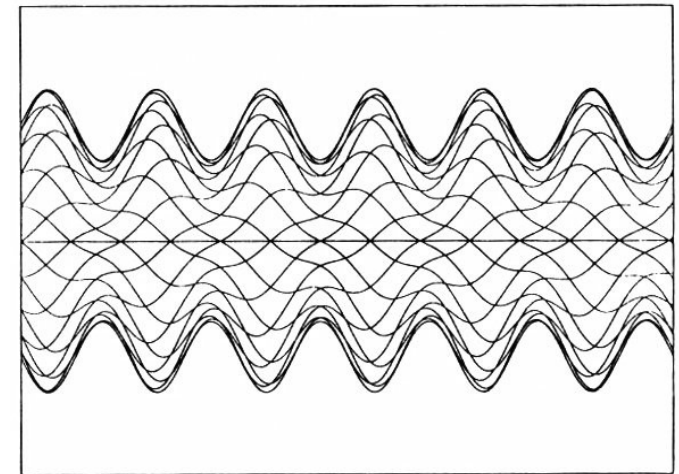
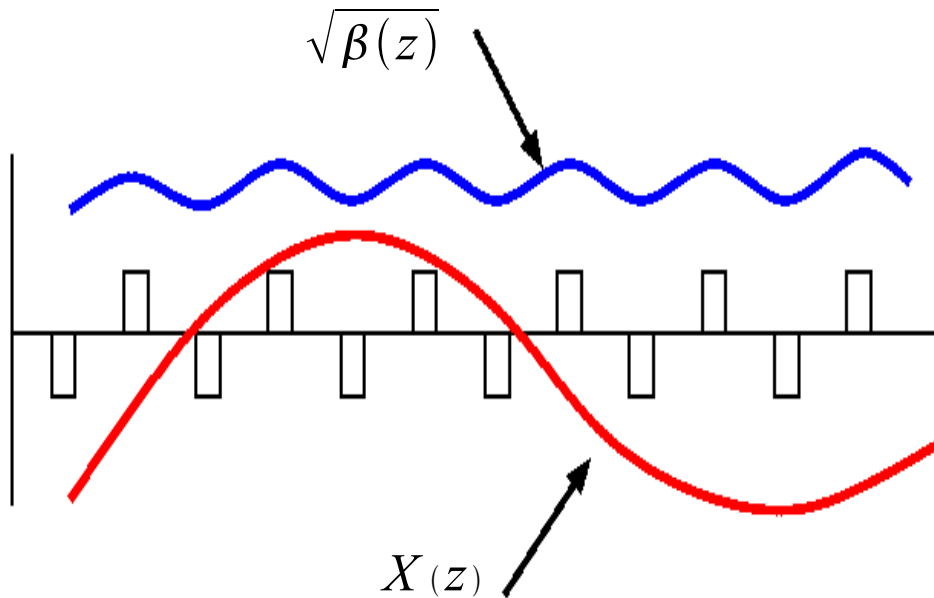
Trajectory of a Single Ray

The solution to Mathieu's equation has the form $x(z) = X(z)\sqrt{\beta(z)}$

Where $X(z)$ is a slowly varying function and $\sqrt{\beta(z)}$ varies with the periodicity of the quads.

$$\beta^2 \lambda^2 \frac{d^2 X(z)}{dz^2} + \sigma^2 X(z) = 0 \quad \sigma^2 = \frac{B^2}{8\pi^2} + \Delta$$

Where σ is the **tune** of the **betatron oscillations** of the ray.



The beam is the ensemble of all the rays within the envelope.

Each ray is the product of the two functions.

Beam Bunching and Beam Capture

In other types of accelerators, such as drift-tube linacs, the beam passes through a single bunching cavity. The energy modulation, after a suitable drift, creates a density modulation, and approximately 50% of the beam may be captured in the accelerating bucket of the linac.

In RFQs, as **the longitudinal field profile can be arbitrarily chosen**, a more sophisticated bunching process can occur, in effect, many smaller bunchers which can together shape the density modulation so that nearly all the beam may be captured in the accelerating bucket.

The design process of an RFQ emphasizes the optimum design of the longitudinal field profile that maximizes capture for a given beam current. The slow, multi-cell bunching process is called *adiabatic* bunching.

The nearly 100% capture of an unbunched beam from the ion source is especially important for ion species difficult or expensive to generate, such as heavy ions.

A further advantage of the RFQ is the use of a **lower injection energy** from the ion source, 25 to 100 kV, compared to that previously used for drift-tube linacs, typically 750 kV.

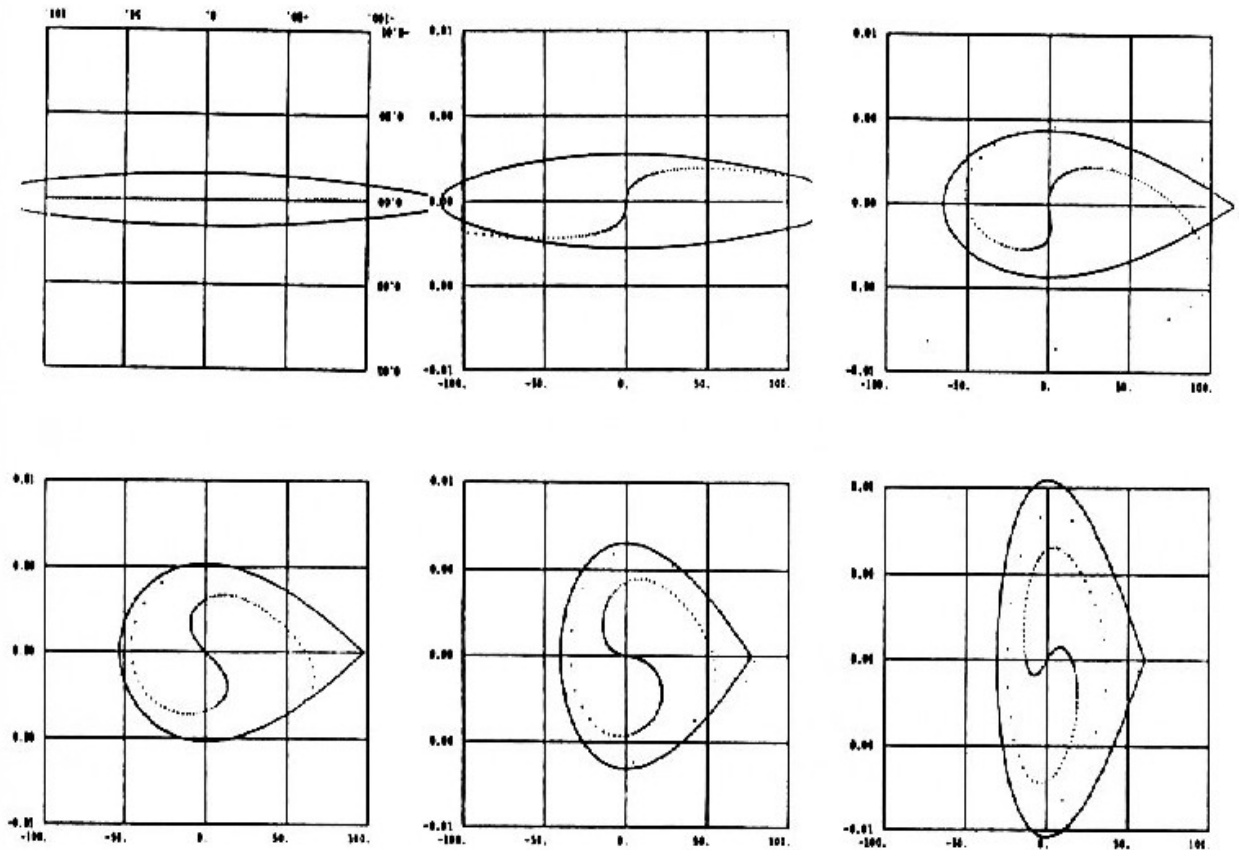
The Bunching Process

The six longitudinal phase space diagrams show the idealized bunching process for a zero-emittance beam with no space charge.

The bunch is subject to a constant but small sinusoidal longitudinal field which produces an energy spread that causes the longitudinal phase space to **filament**, or to wrap around itself.

A separatrix surrounding the bunch grows in (energy) height and collapsed in (phase) length during the bunching process. After several phase oscillations, the majority of the injected beam is concentrated near the center of the separatrix.

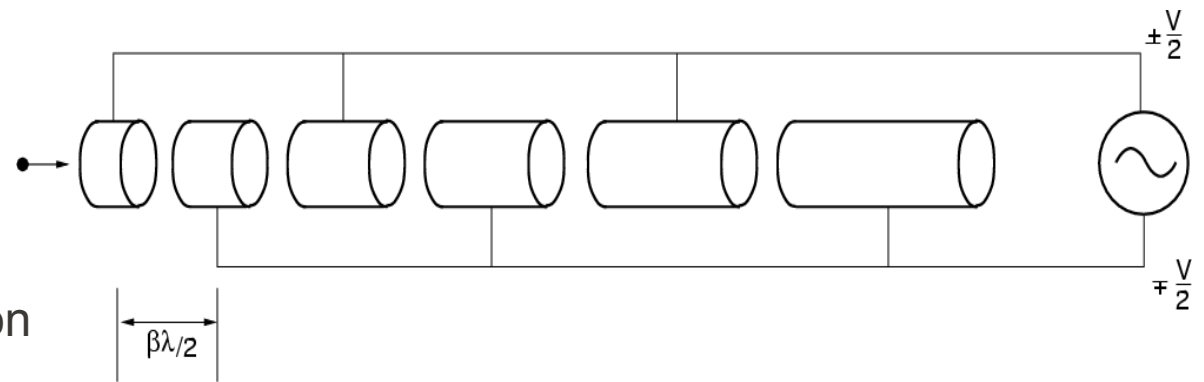
Note that the bunching process produces an energy spread in the beam, which will affect the energy spread of the accelerated beam at the exit of the RFQ.



A Sloan-Lawrence Accelerator

The longitudinal fields in the RFQ are a result of the modulations on the vanetips. Typically, the vanetip potential profile is constant along the structure, resulting in constant focusing strength. As the beam energy increases, the cell length increases as βl , so the accelerating field is the vane potential V divided by b , and therefore drops off as b .

This limits the accelerating efficiency of the structure at high energy. The efficiency of a typical proton RFQ drops off sufficiently at 2-3 MeV, which is an optimum energy to transition to a drift-tube linac.



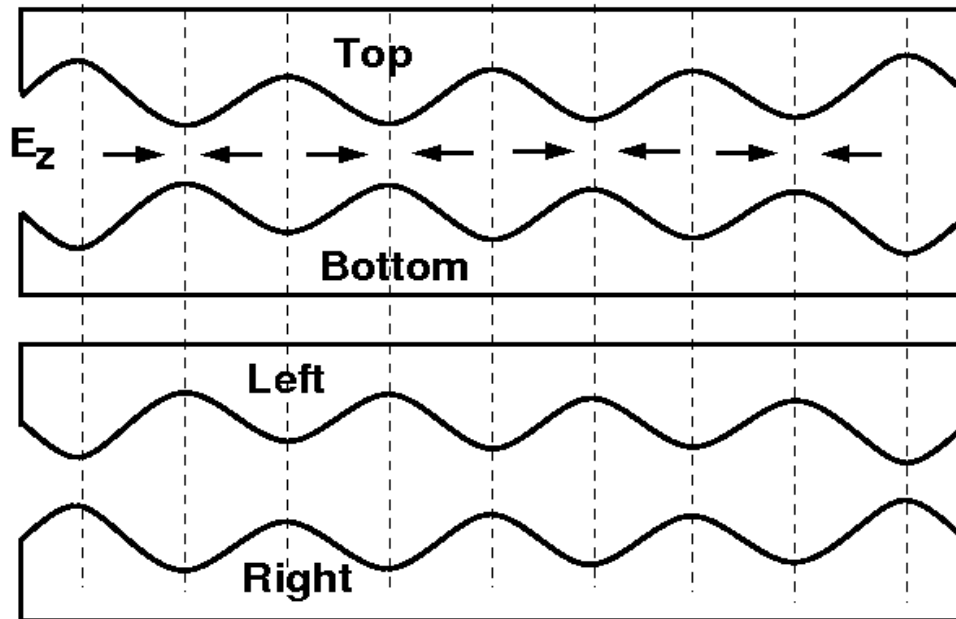
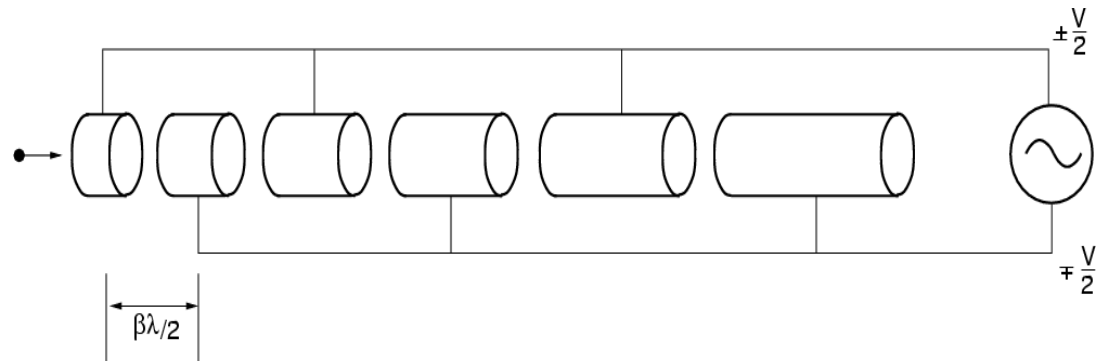
In a typical proton accelerator system, a 50-100 kV ion source will inject an RFQ, which will accelerate the beam to 2-3 MeV, followed by a drift-tube linac, further accelerating the beam to 100-200 MeV, at which point the drift-tube linac efficiency is lower than a more efficient structure, such as a side-coupled linac.

Adding Acceleration to the RFQ

The RFQ starts out as a strong focusing channel, which can transport beams.

To make it into an accelerator, a longitudinal field E_z is introduced.

Recall that in a Sloan-Lawrence accelerator, gaps are separated by $\beta\lambda/2$.



The tips of the poles (vanes) in the RFQ are modulated with wiggles, where the phase of the wiggles in the top and bottom vanes is out of phase of those in the left and right vanes.

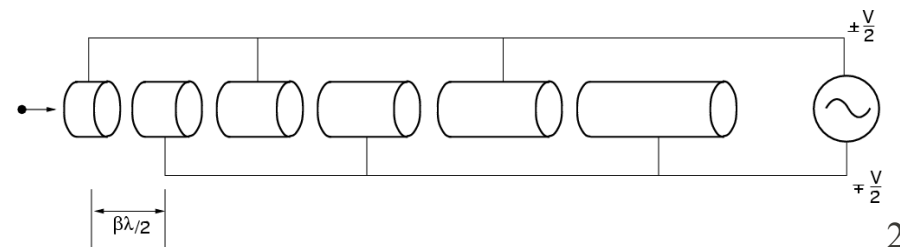
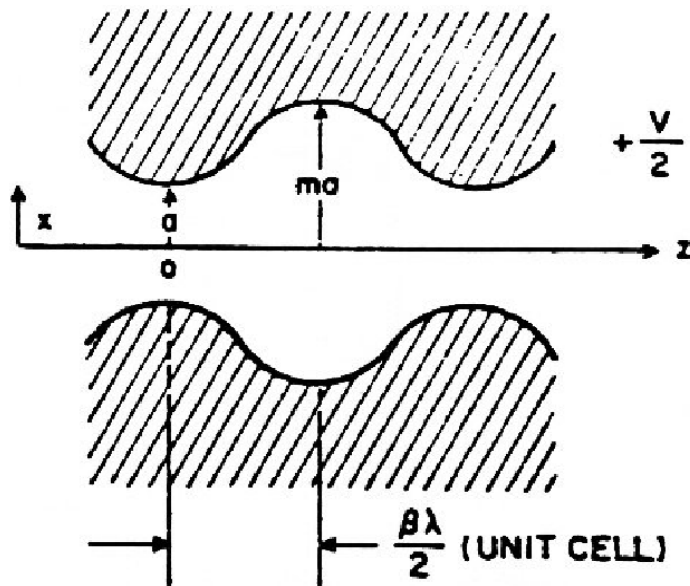
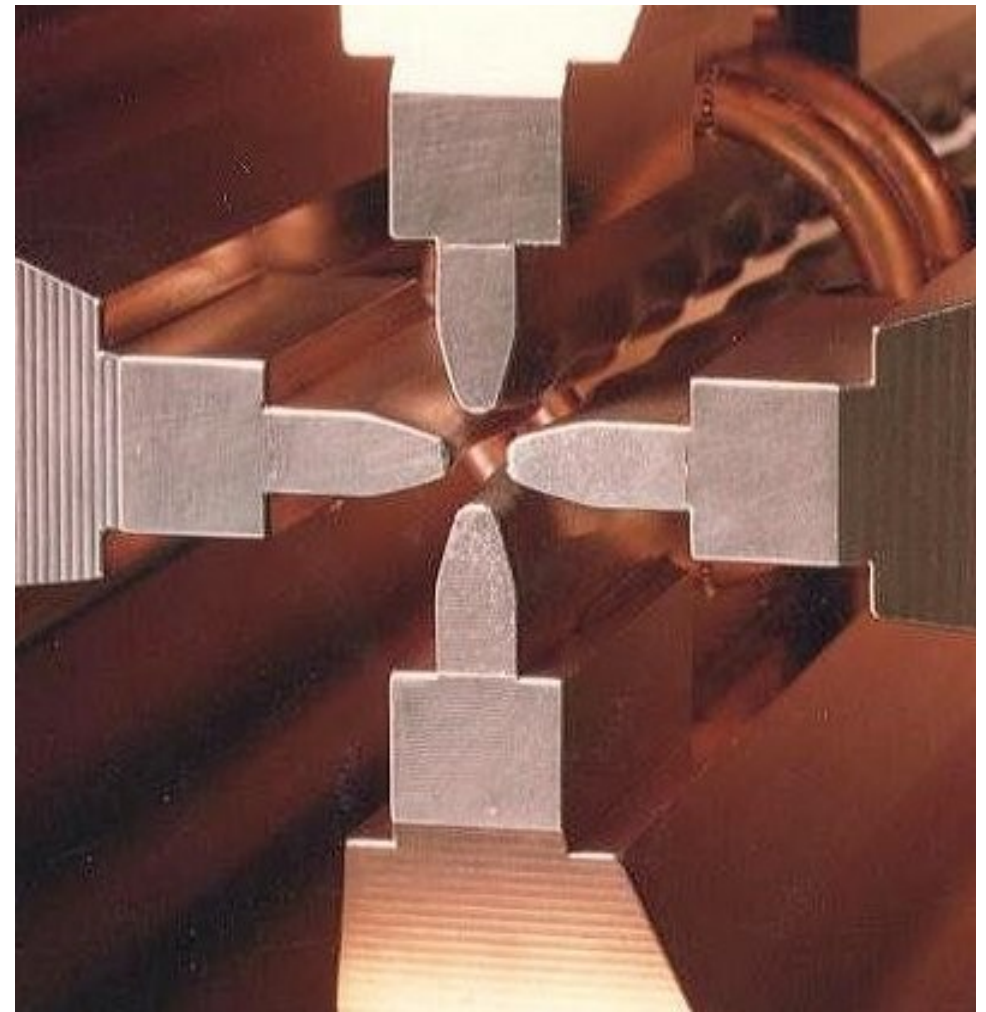
This creates an alternating longitudinal field equivalent to the fields in the gaps of a Sloan-Lawrance accelerator.

Modulated Vanes in an RFQ

The vane tip modulations are visible in the end section of this RFQ.

The spacing between crests is $\beta\lambda$.

An accelerating cell in an RFQ is half the spacing between crests, corresponding to a cell of a Sloan-Lawrence accelerator.



The Vane Tip Modulations

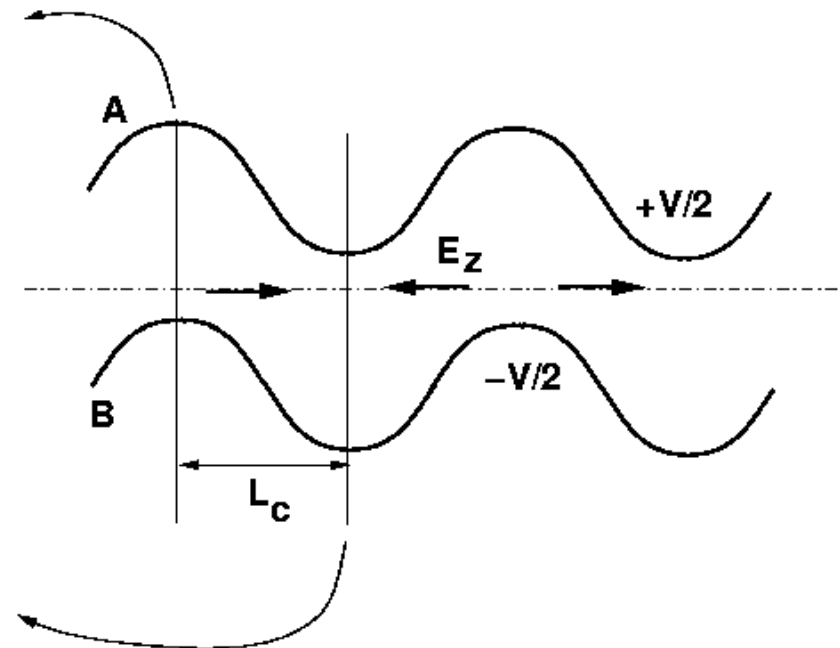
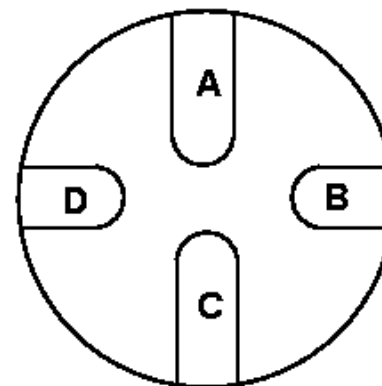
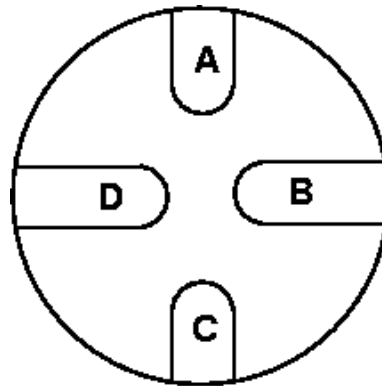
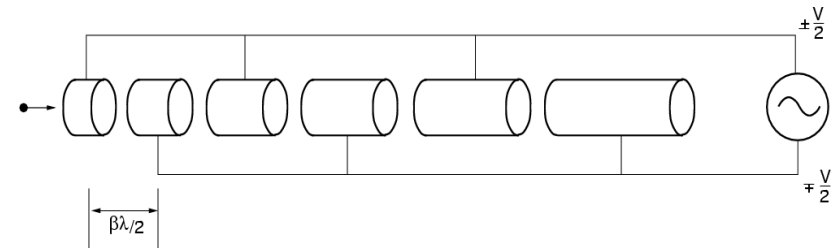
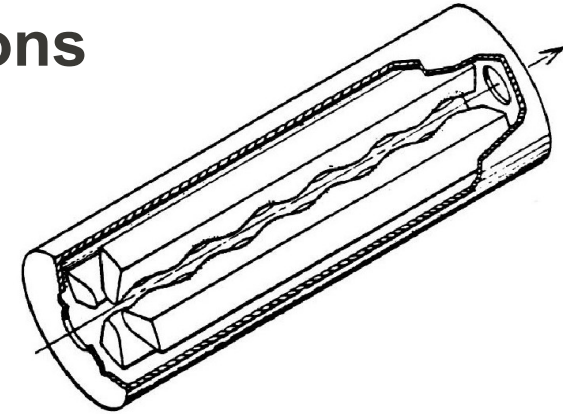
The modulations in the vane tip on the odd vanes are out of phase with the modulations on the even vanes.

The voltage on the odd vanes is out of phase with the voltage on the even vanes.

The vane tip to vane tip voltage is V , so each vane carries a time-dependent voltage of

$$V_{vane} = \pm \frac{V}{2} \sin \omega t$$

A longitudinal field is generated along the axis that depends on the geometry of the modulations. This field accelerates the ions.



Design an RFQ Accelerator

In this section, you will design a RFQ accelerator.

Design the cavity cross section to support the fields

Design the vane tip modulation profile to capture and accelerate the beam

We will use Superfish to design the RFQ cavity structure.

We will use Parmteq to design and simulate the beam dynamics.

The Optimization Procedure

The injection energy of 65 keV is chosen as a compromise between:

Favors lower voltage

Ion Source LEBT sparking

Size and cost of ion source / LEBT

Shorter RFQ (why shorter? The RFQ needs to add *more* energy)

Favors higher voltage

Lower output emittance

Lower space charge dependence

Greater current capability for future expansion

The chosen 65 keV injection energy is as much as an intuitive choice as it is a hard number. It is based on experience with past accelerators and a lot of simulations. Parameters such as reliability are difficult to fold into an optimization procedure. This points out that the design of an accelerator system relies to some extent on unknowables.

In the following pages, a Linux version of Parmteq is used to design the SNS RFQ. A similar design procedure is used with the LANL codes.

Superfish Problem Example for a Complex RFQ

This is the first half of the input file.

Title information

```
RFQ full quadrant
Lowest dipole-mode frequency = 412.043 MHz
Bore radius at quadrupole symmetry point r0 = 0.297 cm
Vane-tip radius of curvature rho = 0.24371 cm
```

```
; Copyright 1998, by the University of California.
; Unauthorized commercial use is prohibited.
```

Region definitions.

```
&reg kprob=1,           ; Superfish problem
; Define X (physical) and K (logical) line regions:
```

Mesh refinement

```
xreg1=0.70, kreg1=50,
xreg2=1.4,  kreg2=80,
xreg3=2.1,  kreg3=95,
kmax=120,
```

```
; Define X (physical) and K (logical) line regions:
```

```
yreg1=0.70, lreg1=50,
yreg2=1.4,  lreg2=80,
yreg3=2.1,  lreg3=95,
lmax=120,
```

icylin=0 for RFQ

freq= 412.043

rfq=1

left-hand boundary

```
icylin=0,           ; Cartesian coordinates
freq=412.04344,     ; Starting frequency
dslope=-1,         ; Allow convergence in one iteration
rfq=1,             ; Cavity type is RFQ
; The following line is for dipole modes; use nbslf=0 for quadrupole modes
nbslf=1,           ; Neumann boundary condition at left edge
lines=0 &         ; allow line region points to move in mesh optimization
```

Superfish Problem Example for a Complex RFQ

This is the last half of the input file.

The control point contain a number of straight line segments and arcs.

```
&po x=0.,y=0. &  
&po x=0.,y=.297 &  
&po nt=2,x0=0.,y0=.54071,y=-0.04232,x=.24001 &  
&po x=.342,y=1.07680 &  
&po x=.342,y=2.0 &  
&po x=1.0253,y=3.8734 &  
&po x=1.7267,y=5.7469 &  
&po x=2.428,y=7.6203 &  
&po x=2.428,y=7.7274 &  
&po nt=2,x0=3.063,y0=7.7274,x=0.,y=.635 &  
&po x=3.4638, y=8.3624 &  
&po x=8.3624, y=3.4638 &  
&po x=8.3624, y=3.0630 &  
&po nt=2, x0=7.7274, y0=3.0630,x=0.,y=-.635 &  
&po x=7.6203, y=2.428 &  
&po x=5.7469, y=1.7267 &  
&po x=3.8734, y=1.0253 &  
&po x=2.000, y=.3420 &  
&po x=1.07680,y=.342 &  
&po x=.49839, y=.24001 &  
&po nt=2,x0=0.54071,y0=0.,x=-.24371,y=0. &  
&po x=0.,y=0. &
```

The .SEG file for the problem.

```
NormalizationCode= 0 ; NORM, normalize fields to  
EZERO  
E0 = 11.207e6 ; EZERO, in Volts/meter  
FieldSegments  
2 3 4 5 6 7 8 9 10 ; Start of segment numbers  
11 12 13 14 15  
16 17 18 19 20  
21 22 23 24 25  
26 27 28 29 30 31 32  
EndData  
End
```

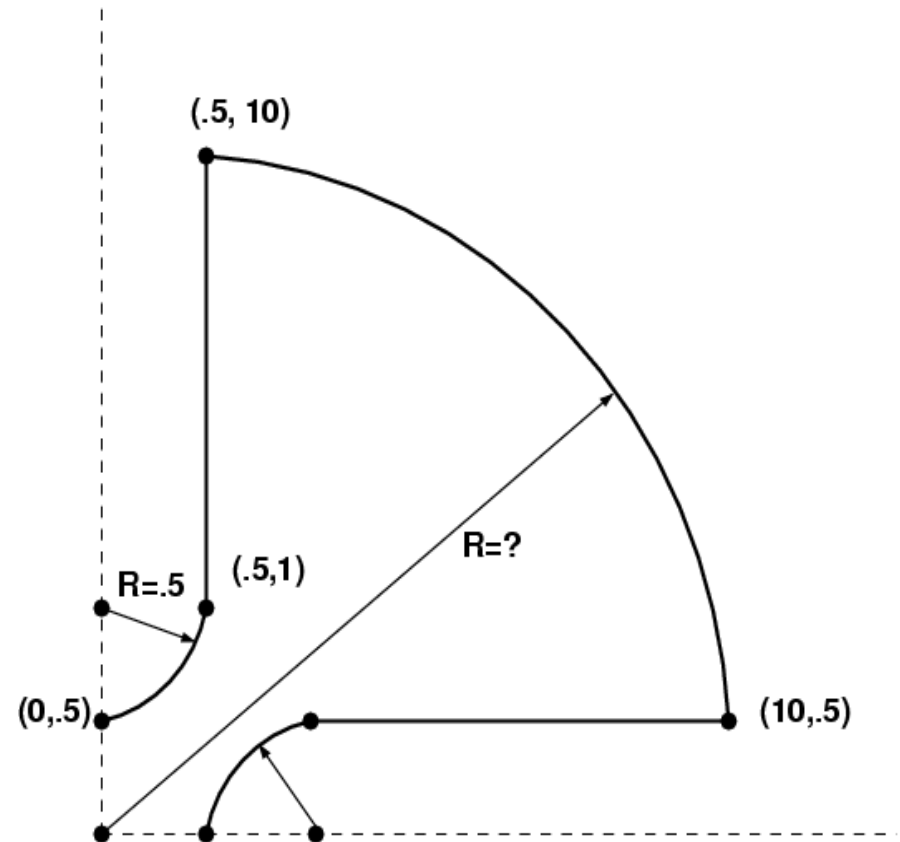
Problem: Solve a Simple RFQ

We will solve a very simple geometry, and then use a spread sheet to calculate a more complex geometry.

The RFQ will have vane tips with a radius of 0.5. The outer shell will pass through the points $(0.5, 10)$ and $(10, 0.5)$, drawn by an arc whose center is at the origin. (What is the radius of the arc?)

Take the example file 4THRFQ.AF and generate a file RFQ1.AF that describes this geometry. Include a mesh size change at $x=1.3$ cm and $y=1.3$ cm.

We will solve for both the quadrupole mode and the dipole mode (in file RFQ2.AF).



Input File for RFQ1.AF

```
RFQ1, Simple, quadrupole mode

; Copyright 1998, by the University of California.
; Unauthorized commercial use is prohibited.

&reg kprob=1,           ; Superfish problem
xreg1=1.30, kreg1=20,
kmax=60,
yreg1=1.30, lreg1=20,
lmax=60,
icylin=0,             ; Cartesian coordinates
freq=300.0,          ; Starting frequency
rfq=1,               ; Cavity type is RFQ
nbslf=0,             ; Boundary condition at left edge for quadrupole
lines=0 &           ; allow line region points to move in mesh optimization

&po x=0.,y=0. &
&po x=0.,y=.5 &
&po nt=2,x0=0.,y0=1.0,x=0.5,y=0 &
&po x=.5,y=10.0 &
&po nt=2,x0=0,y0=0,x=10.,y=.5 &
&po x=1.0, y=0.5 &
&po nt=2, x0=1.0, y0=0.0,x=-0.5,y=0.0 &
&po x=0.,y=0. &
```

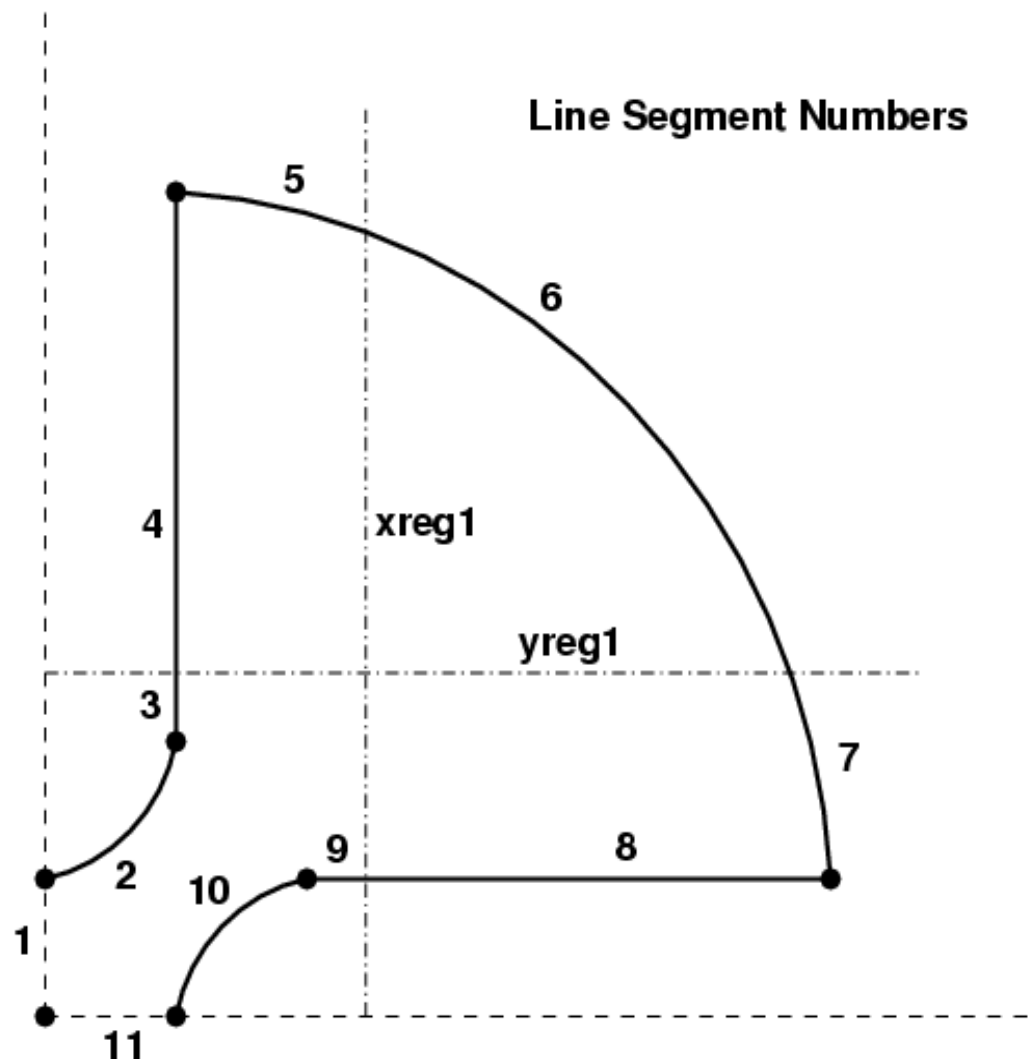
Segment Numbering for RFQ1.AF

The mesh refinement at $x=1.3$ and $y=1.3$ (xreg1 and yreg1) divide the boundary of the problem into 11 segments.

The power will be calculated separately on each segment.

Which segments do we **not** want to calculate power on? (They are not metallic.)

What is the quadrupole mode frequency? How do you know that it is the quadrupole mode, from looking at the field plot?



Dipole Mode for RFQ2.AF

```
RFQ2, Simple, dipole mode
```

```
; Copyright 1998, by the University of California.  
; Unauthorized commercial use is prohibited.
```

```
&reg kprob=1,           ; Superfish problem  
xreg1=1.30, kreg1=20,  
kmax=60,  
yreg1=1.30, lreg1=20,  
lmax=60,  
icylin=0,             ; Cartesian coordinates  
freq=300.0,          ; Starting frequency  
rfq=1,               ; Cavity type is RFQ  
nbslf=0,             ; Boundary condition at left edge for dipole  
lines=0 &           ; allow line region points to move in mesh optimization
```

```
&po x=0.,y=0. &  
&po x=0.,y=.5 &  
&po nt=2,x0=0.,y0=1.0,x=0.5,y=0 &  
&po x=.5,y=10.0 &  
&po nt=2,x0=0,y0=0,x=10.,y=.5 &  
&po x=1.0, y=0.5 &  
&po nt=2, x0=1.0, y0=0.0,x=-0.5,y=0.0 &  
&po x=0.,y=0. &
```

RFQ Dipole and Quadrupole Mode Frequencies

The TE_{210} frequency for this problem is about 320.5 MHz, and the TE_{110} frequency is about 310 MHz. Because this structure is symmetric without errors, as calculated, there will be another TE_{110} mode with the fields rotated 90 degrees from the one calculated.

The TE_{110} and TE_{210} modes are closely spaced, and construction errors may bring them even closer.

We can estimate the effect of construction errors using additional information in the output (SFO) file.

Segment Frequency Sensitivity List

The SFO analysis program lists the sensitivity of the resonant frequency to perturbations in the position of each segment. The perturbation is calculated for each segment moved in the x- and in the y-direction by 1 millimeter. Some segments, such as segments 3 and 4, which are vertical line sections, will cause no perturbation if moved in the y-direction. The vane tips, segments 2 and 10, cause a significant frequency perturbation.

(Caution, segment 2 moving along x is to be interpreted as a fattening of the segment, not just a transverse move, for example) On the basis of this data, the thermal response of the RFQ is calculated and the cooling passages specified.

Wall segments:

Segment	Xend (cm)	Yend (cm)	E _{max} (MV/m)	Power (mW)	P/A (mW/cm ²)	dF/dX (MHz/mm)	dF/dY (MHz/mm)
	0.0000	0.50000					
2	0.50000	1.0000	2.723	6.804	8.670	13.09	13.96
3	0.50000	1.3000	1.453	8.780	29.27	1.584	0.000
4	0.50000	10.000	0.8450	636.4	73.15	0.1730	0.000
5	1.3000	9.9277	3.1605E-03	69.81	86.89	-1.8476E-02	-0.2046
6	9.9277	1.3000	3.5617E-03	1138.	86.70	-2.201	-2.201
7	10.000	0.50000	2.7244E-03	69.81	86.88	-0.2045	-1.8476E-02
8	1.3000	0.50000	0.8110	636.4	73.15	0.000	0.1551
9	1.0000	0.50000	1.450	8.778	29.26	0.000	1.626
10	0.50000	0.0000	2.714	6.823	8.694	14.00	13.04
Total				2581.			

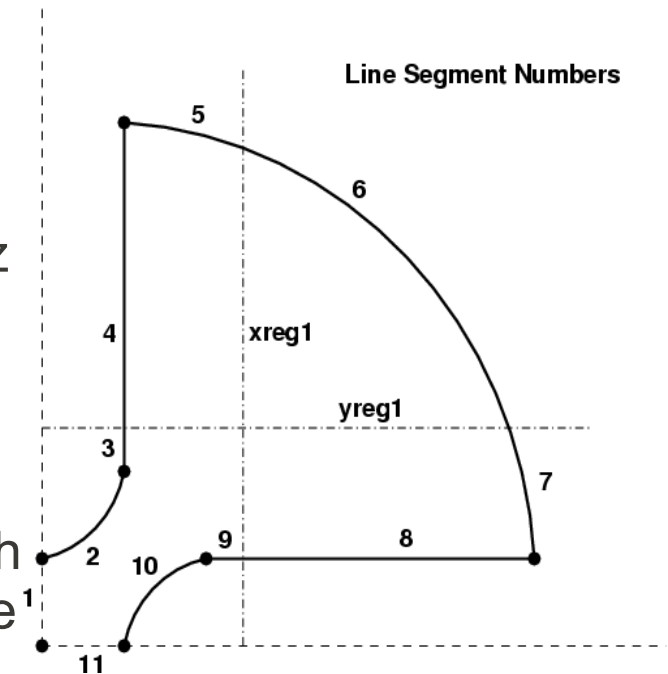
Problem: Solve for Vane Radial Displacement Tolerance.

Segment	Xend (cm)	Yend (cm)	E _{max} (MV/m)	Power (mW)	P/A (mW/cm ²)	dF/dX (MHz/mm)	dF/dY (MHz/mm)
2	0.50000	1.00000	2.723	6.804	8.670	13.09	13.96
...							
10	0.50000	0.00000	2.714	6.823	8.694	14.00	13.04

Segment 2 (end of vertical vane) shows a frequency sensitivity of 13.96 MHz per mm vertical displacement.

Segment 10 (end of horizontal vane) shows 14.00 MHz per mm of horizontal displacement. (Why are the sensitivities different?)

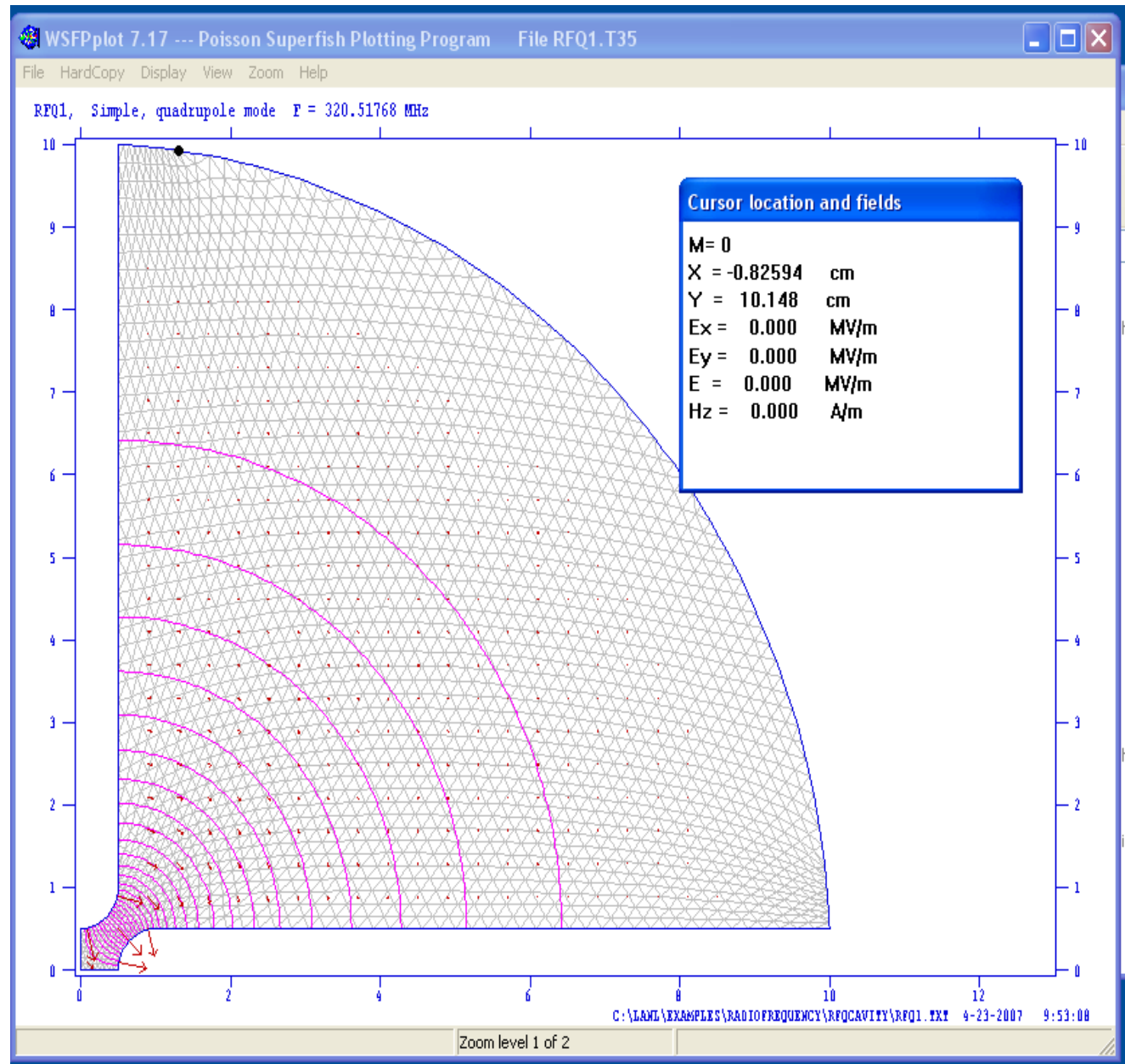
The RFQ frequency is 320.5 MHz. If the construction of the RFQ has a consistent error of the lengths of each vane, what total error would cause a 1% lowering of the RFQ frequency?



Graphical Output of Simple Example

This plot shows the mesh, the contour lines, and the arrows.

The inset shows the fields at the position of the cursor.



The Four RFQ Sections (LANL Design Procedure)

LANL has derived a “cookbook” RFQ design, based on the PARMTEQ code, written at LANL. This design procedure divides the RFQ into four segments, each with a particular function. This design procedure was first introduced by the inventors of the RFQ, Kapchinskii and Teplyakov.

These segments are:

Radial Matcher: Takes the DC beam from the ion source with constant radius and transforms it into a beam that matches the strong alternate-gradient focusing pattern in the RFQ

Shaper: Starts the bunching process

Gentle Buncher: Continues the bunching process until the beam is fully bunched and slightly accelerated. The stable phase has been reached.

Accelerator: Applies full accelerating field and takes the beam to full energy.

An adiabatic buncher in the true sense would be infinitely long, so the shaper gets the bunching process started and then hands it off to a finite-length buncher.

The PARMTEQ Group of Codes

The PARMTEQ code, written at LANL, is used by most RFQ designers in the United States and elsewhere. Many other RFQ design codes have appeared based on more modern coding methods that contain a more detailed physics simulation, but PARMTEQ remains an important code.

The PARMTEQ code receives from additional helper codes the description of each cell in a proposed RFQ. PARMTEQ generates the RFQ accelerator cell table and the fields in each cell.

PARMTEQ then generates or inputs an ensemble of macroparticles representing the beam to be accelerated. An actual bunch may contain 10^9 or more ions. A simulation with 10^9 ions would tax present computers, so a smaller number of macroparticles are generated with the same statistics (size, emittance) as the bunch, but each carrying a charge and mass that produces the same value of beam-beam space charge interaction as the actual particles in the bunch.

The bunch of macroparticles is tracked through the cells and the statistics of the beam (size, energy, emittance, particle loss) is recorded for later inspection.

This process is iterated until an acceptable solution is found.

The CURLI Code

The RFQ design process consists of first evaluating the beam stability at the most critical point in the RFQ, the end of the gentle buncher. Here, the beam bunch is fully formed and has been accelerated slightly over the injection energy.

The space-charge forces are the strongest at this point. The betatron tune is depressed due to the space-charge forces which counteract the alternating-gradient external electric quadrupole restoring force. Enough space-charge tune depression can bring the tune to zero, rendering the beam unstable.

The beam dynamics at the energy chosen at the end of the gentle buncher is evaluated with the **CURLI** code. The parameters chosen include:

energy, vanetip voltage, beam aperture

with the desired input variables

frequency, beam current, peak surface field.

The RFQUICK Code

After the cell at the end of the gentle buncher is designed, the cell table for the rest of the RFQ is generated using RFQUICK.

The last task is to select the energy at the beginning of the gentle buncher, which is the same as the energy at the end of the short shaper section.

RFQUICK will estimate the length of the generated RFQ, its RF power demand, and the capture fraction of the input beam and longitudinal emittance of the beam at the exit of the RFQ.

The PARI Code

Historically, the first RFQs were generated using the two-term potential to calculate the beam trajectories. These RFQs worked, but the measured performance did not fully meet expectations. A major contributor was the truncation of the field equations to two terms.

Adding six more terms (and later two more for off-axis trajectories) significantly improved the agreement between simulated and measured performance.

$$\begin{aligned} \frac{2}{V} U(r, \theta, z) = & A_{01} \left(\frac{r}{r_0} \right)^2 \cos 2\theta + A_{03} \left(\frac{r}{r_0} \right)^6 \cos 6\theta + A_{10} I_0(kr) \cos kz \\ & + A_{12} I_4(kr) \cos 4\theta \cos kz + A_{21} I_2(2kr) \cos 2\theta \cos 2kz + A_{23} I_6(2kr) \cos 6\theta \cos 2kz \\ & + A_{30} I_0(3kr) \cos 3kz + A_{32} I_4(3kr) \cos 4\theta \cos 3kz \end{aligned}$$

PARI takes the two-term cell table generated with RFQUICK and calculates the fields with the 8-term potential. It then modifies the aperture \mathbf{a} and modulation parameter \mathbf{m} for each cell so the synchronous particle is kept in synchronism with the RF phase.

The PARMTEQ Code

The CURLI and RFQUIK programs generate files that are used by the PARMTEQ program to generate an ensemble of particles simulating a bunch and then track them through the RFQ to the end.

A complete record of the coordinates of each macroparticle in each cell is kept in a large file for subsequent analysis.

The PARMTEQ program works by generating the fields for each cell in the RFQ and integrating the particle trajectories through the cell. If a particle's trajectory is large enough to hit the tip of the RFQ vane, it is flagged as lost. If the energy of a macroparticle exceeds a specified value, it is also flagged and lost.

PARMTEQ calculates the space-charge interaction among the macroparticles in the bunch, including adjacent bunches, with the SCHEFF subroutine.

The SCHEFF Subroutine

It is important to understand how SCHEFF works.

Each macroparticle in the bunch interacts with all others.

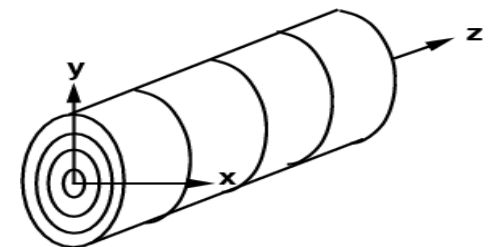
The force between two charges separated by r is:

$$F = \frac{q_1 q_2}{4\pi \epsilon_0 r^2}$$

For N macroparticles, $N^2/2$ calculations would be required to calculate all the interactions, and this would be repeated for each cell in the RFQ. This is numerically intensive, and not fully accurate as it does not correctly account for very close-range interactions.

Instead, a computationally efficient algorithm is used, a variation of Particle-In-Cell (PIC) calculation is used. Here, the bunch is divided into a series of annuli (rings) radially, and slices longitudinally. The charge contained in the macroparticles in each annulus is distributed in each and added up for all charges.

After the charge is deposited in each of the annuli, The fields are calculated using look-up tables of elliptic integral functions and used to give a kick to each macroparticle. The size of the mesh is adjusted for each cell so it encloses the bunch.



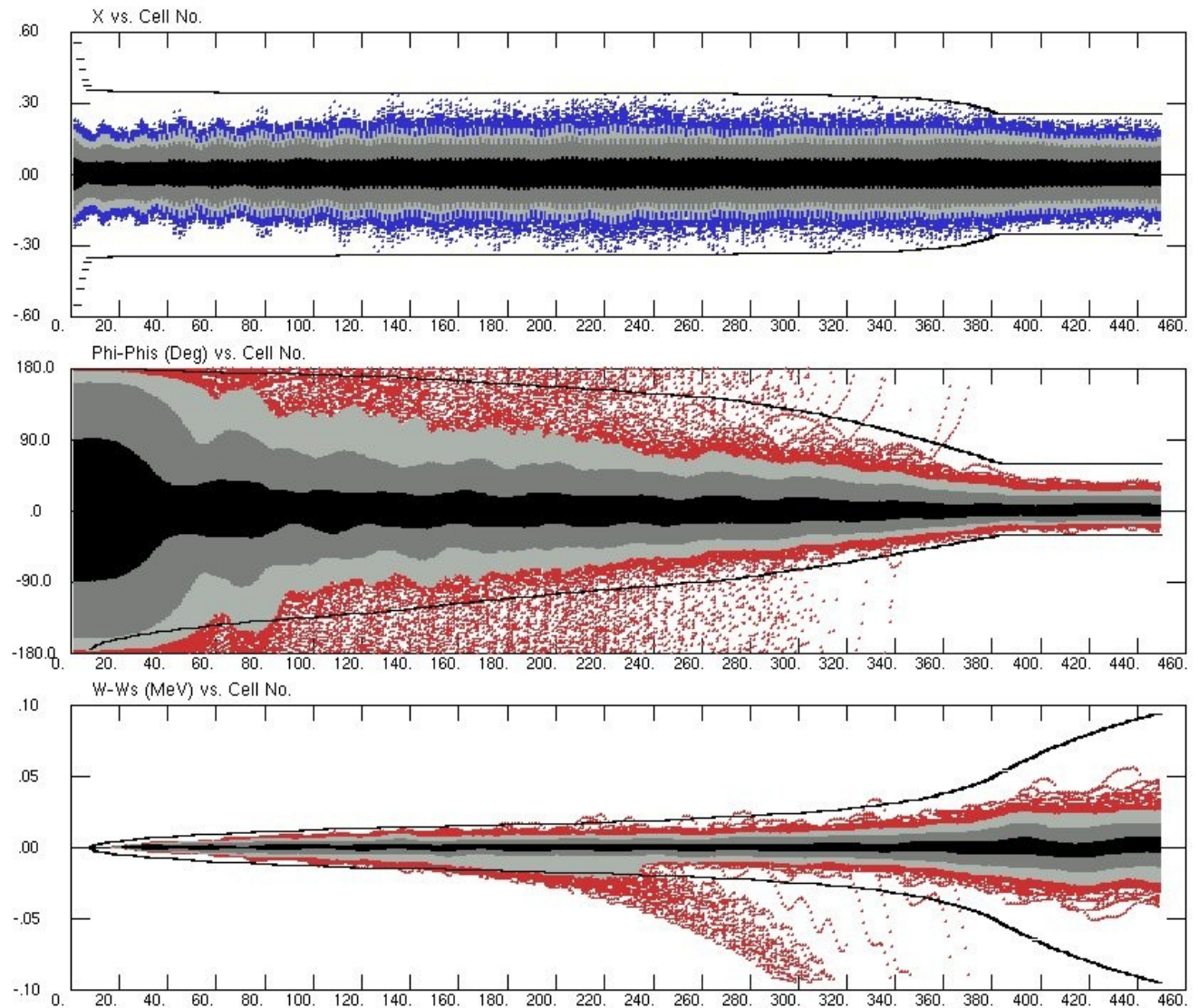
As this approach assumes that the bunch is cylindrically symmetric, the SCHEFF algorithm is applied at the midpoint of the RFQ cell, where the beam is most likely round. In practice, the SCHEFF algorithm give results comparable to a much slower 3-D calculation.

The WSFLOT Plotting Code

Once the PARMTEQ program has tracked each macroparticle in the bunch through the RFQ and save the coordinates of each particle in each cell, the [wsfplot](#) program is used to analyze the results.

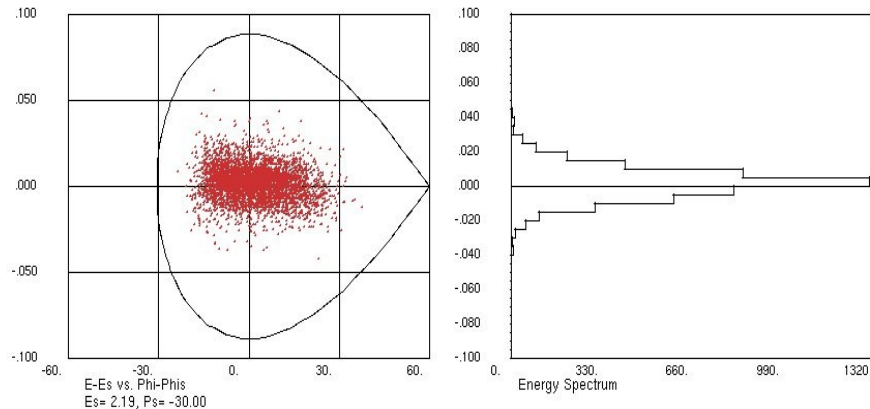
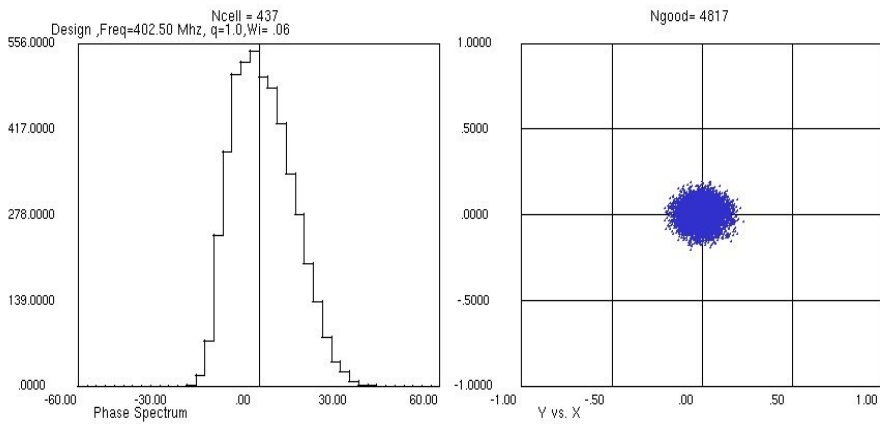
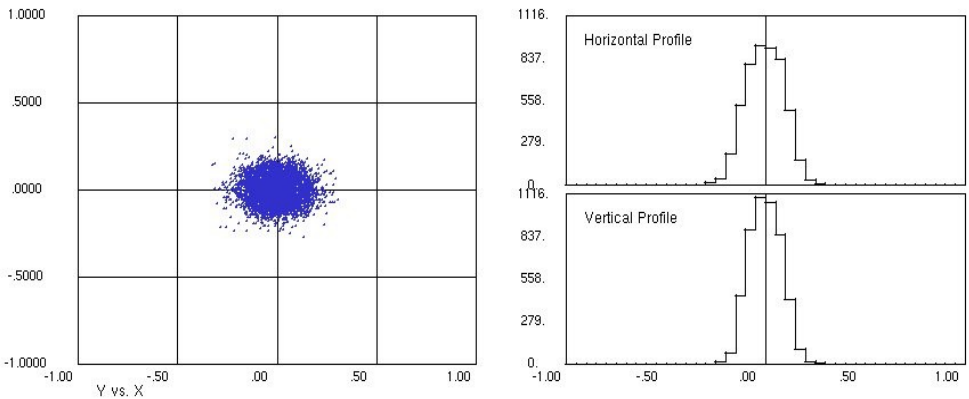
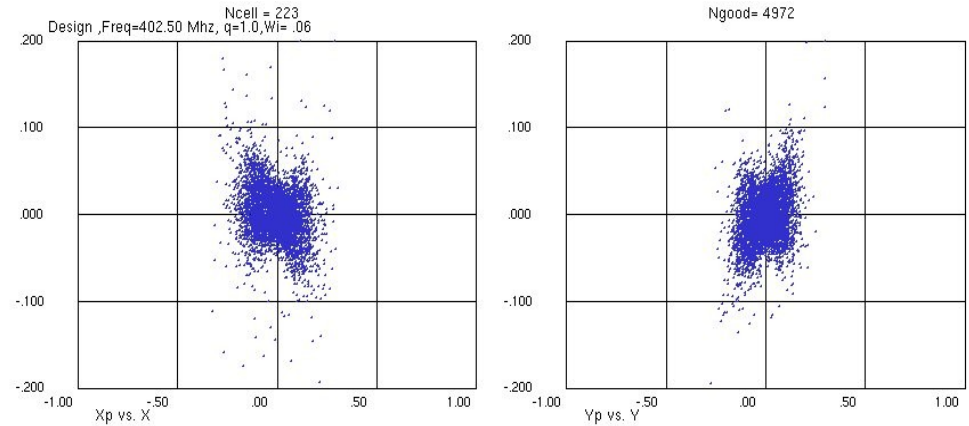
The trajectories of all particles can be plotted in each cell. Here, the x-coordinate of each particle is plotted in each cell of the SNS RFQ, along with the phase and energy deviation from the synchronous particle in each cell.

The colors represent the 50%, 90% and 98% contours of the particle number in the bunch.



More wsfplot Plots

The plot on the right shows both the $x-x'$ and $y-y'$ phase space, along with the $x-y$ distribution and histograms of the x and y profiles.



The plot on the left shows the longitudinal phase space (energy vs. phase), along with the surrounding separatrix. Also plotted is again the $x-y$ distribution and histograms of the energy and phase distribution for cell 437 of the SNS RFQ, near the end.

Ion Sources for RFQs

The RFQ accepts positive (or negative) ion from the ion source and the Low Energy Beam Transport (LEBT) system. The LEBT transports the beam and matches it to the input phase space requirement of the RFQ.

The LEBT may use magnetic solenoid or quadrupole focusing, or may use electrostatic (Einzel) lens focusing. The ability to steer the beam into the RFQ is usually provided.

A pulsed ion source generates a beam which may be varying in time. Often, the beginning of the pulse is not in equilibrium with the rest of the pulse as the ion source may not stabilize quickly or space-charge neutralization has not yet taken effect in a magnetic LEBT. The initial part of the beam pulse may not be well matched to the RFQ acceptance and therefore suffers higher loss in the RFQ.

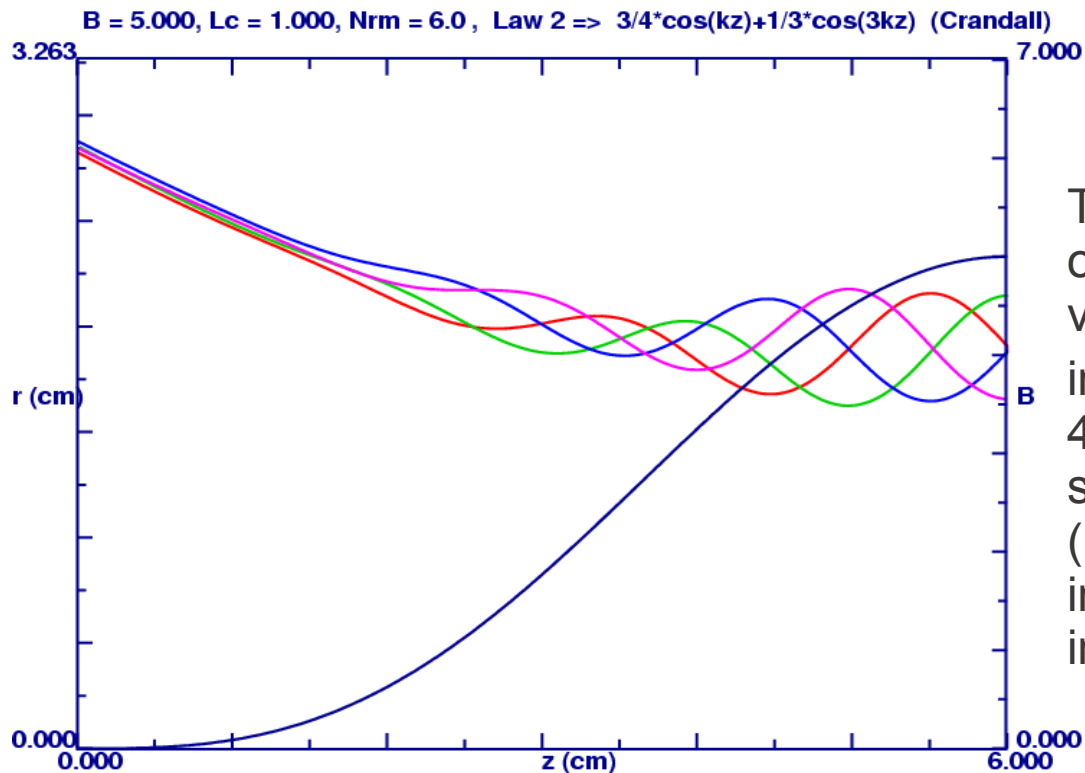
The transverse beam properties are constant in time and must be transformed into a time-varying envelope once inside the RFQ. This transformation takes place in the **radial matcher**.

The Radial Matcher

The radial matcher section of the RFQ transforms a constant beam cross-section to a time-varying cross section that matches the time-varying focusing force in the RFQ.

The focusing strength B_0 is proportional to $1/a^2$, a is the distance of the vane tip from the axis.

$$B_0 = \left(\frac{qeV}{mc^2} \right) \frac{\lambda^2}{a^2}$$



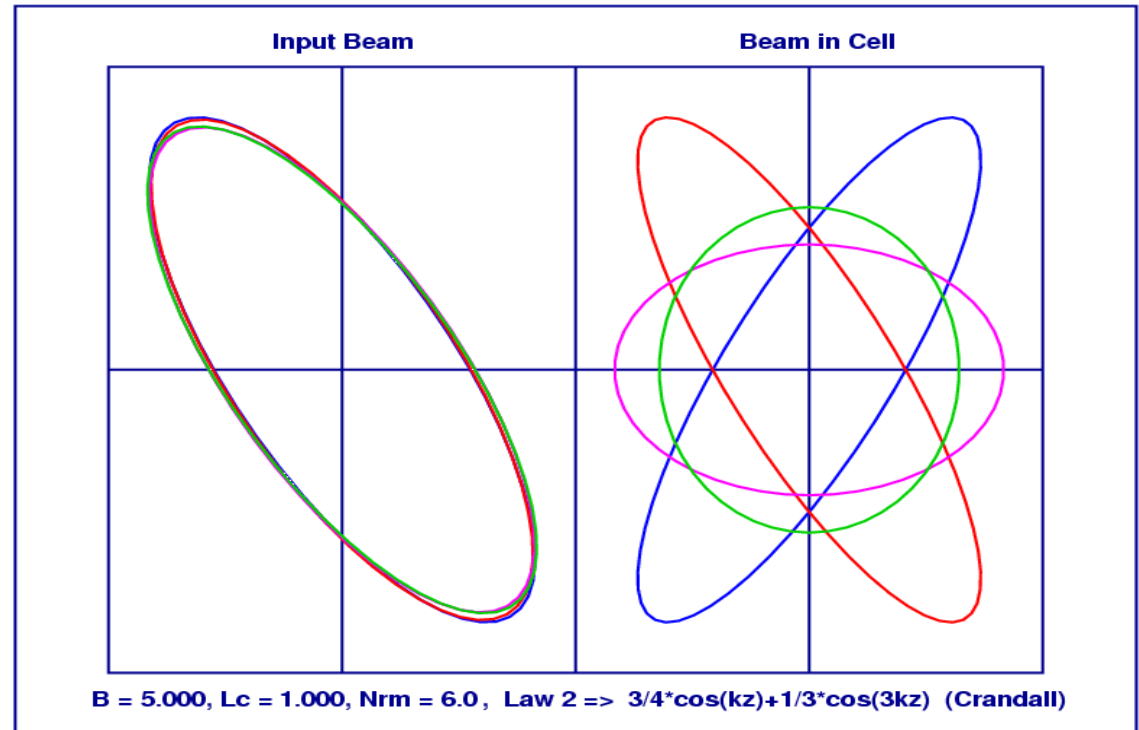
The radius a of the vanetips from the start of the vane is tapered inward to the final value r_0 . The focusing parameter B_0 increases, and the beam envelope for 4 phases of RF (0, 90, 180, 270) degrees shows the transition from constant (no RF phase dependence) to matched into the phase-dependent envelope inside the RFQ.

Phase Space Representation of the Radial Matcher

The phase space diagram shows four beam plots, each for a different RF phase in the RFQ (0,90,180,270 degrees.)

The beam on the left is from the ion source and is not varying in time.

The phase space of the beam shown on the right at four RF phases shows that the beam varies from diverging to converging, and two upright ellipses.



The transformation from a steady beam to one where the envelope is matched to the time-varying RF field takes place in the radial matcher (RM). The RM is typically about 6 cells long, and the radius of the RFQ vanes starts at a large value and tapers down to the final radius from the axis r_0 in the unmodulated vane.

The profile of B_0 is non critical: the one shown here is $B(z) = B_0 \frac{3}{4} \left(\cos(kz) + \frac{1}{3} \cos(3kz) \right)$ (z measured from the *end* of the radial matcher to its beginning.)

Matched Input Beam to RFQ

RFQUICK will suggest the Twiss parameters for an input beam that will match into the RFQ. Space charge forces are included in the estimate.

This suggested beam configuration is usually quite satisfactory, but improved performance may be obtained by making small variations in the beam parameters, or increasing the number of particles in the bunch.

Many bunch distributions are available, such as KV, waterbag, gaussian or others. Measured ion source beam profiles may be introduced instead of using the particle generator contained in PARMTEQ.

The KV (Kapchinsky-Vladimirsky) distribution has a uniform density in 3-space and is the only distribution that has linear space charge fields, which can then be computed analytically. It is an unrealistic distribution, and the other distributions provided reflect more realistically actual distributions provided by ion sources, but the fields are nonlinear.

Nonlinear fields result in emittance growth. A large part of optimization is the selection of RFQ parameters that maximize acceptance and transmission in the RFQ and minimize emittance growth.

Input to CURLI, 1

These are the parameters at the end of the gentle buncher, the beginning of the accelerator section.

First set of inputs:

Mass 1
 Charge 1 (not -1)
 Type 1 means design an RFQ
 f_s -30 degrees
 Current 70 mA (twice desired)

Second set of inputs:

Frequency 402.5 MHz
 Inj energy 0.065 MeV
 Final energy 2.5 MeV

Third set of inputs:

GB end energy 0.75 MeV
 Surface Field 1.85 kilpatrick

The third set is a result of many previous trials of the simulated performance. The energy of 0.75 MeV at the GB exit is a result of these simulations.

Enter Mass(amu),Q,IType(1=>RFQ,2=>pi-pi Wid,3=>pi-3pi Wid,4=>DTL
 Phis(deg),current(mA) 1.0000 1.0000 1 -30.0000 70.0000

Psi,maximum (wg/wi)= 90.9 15.694

Enter Freq(MHz), Wi(MeV), Wfinal(MeV) 402.5000 .0650 2.5000

Enter Wgb(MeV) < 1.02 MeV, Esurface(kilpatrick) 0.75 1.85

.7500 MeV, 36.0183 MV/m, 1.8500 kilpatrick

Enter (1,a(cm),m,dm,nsteps) to find It,Il or (2,0,a,da,nsteps) to set It=Il

2 .0000 .2000 .0100 20.0000

Beta= .04013 Wavel= 74.48 Beta*lambda= 2.989 Bz= .249

n	a	m	A	r0	V	B	dwdz	sig0	del	ani/pi	si/s0	kilp	cx
1	.200	1.987	.556	.309	.075	4.670	1.891	26.1	.068	.115	.598	1.850	.091
2	.210	1.937	.537	.318	.077	4.515	1.870	25.0	.068	.127	.616	1.850	.095
3	.220	1.887	.517	.326	.078	4.377	1.841	24.0	.067	.139	.635	1.850	.099
4	.230	1.837	.497	.334	.080	4.254	1.803	23.2	.065	.151	.653	1.850	.102
5	.240	1.794	.478	.342	.081	4.132	1.769	22.4	.064	.163	.667	1.850	.106
6	.250	1.756	.461	.351	.083	4.010	1.740	21.5	.063	.174	.678	1.850	.109
7	.260	1.719	.443	.359	.085	3.899	1.705	20.7	.062	.185	.688	1.850	.112
8	.270	1.681	.425	.367	.086	3.798	1.664	20.1	.060	.198	.700	1.850	.115
9	.280	1.650	.409	.376	.088	3.694	1.630	19.3	.059	.208	.707	1.850	.118

Enter line number of parameter choice to print out and exit, or 0 to repeat 6

Beta= .04013 Wavel= 74.48 Beta*lambda= 2.989 Bz= .249

n	a	m	A	r0	V	B	dwdz	sig0	del	ani/pi	si/s0	kilp	cx
1	.250	1.756	.461	.351	.083	4.010	1.740	21.5	.063	.174	.678	1.850	.109

Enter I(mA) to track at , 6 x enorm(cm-mrad,n/pi (dist 6)) 60.000 .120

1.0000 1.0000 402.5000 .0650 .7500 2.5000 .0830
 4.0104 .4606 -30.0000 -30.0000 60.0000 .1200 8 .4606

Kilpatrick Criterion

High surface electric fields in a cavity can lead to **electron emission** and **sparking**. Experiments carried out 50 years ago led to an empirical criterion of the safe surface field limit in a cavity, above which electrical breakdown was probable. The cavities were provided with oil-pumped vacuum systems, unlike the clean organics-free vacuum system we use today.

Kilpatrick established his formula for a safe surface field as a function of RF frequency. The equation is in implicit form:

$$f [MHz] = 1.64 E^2 e^{-8.5/E}$$

<u>Freq [MHz]</u>	<u>E [MV/m]</u>
200	14.7
400	19.4
1300	32.1

where the electric field E is expressed in units of MV/m.

It is known that this formula significantly underestimates the sparking limit at frequencies lower than 200 MHz. At higher frequencies, the criterion scales approximately as $f^{0.4}$.

Today, with much cleaner vacuum systems, cavities are operated at much higher surface electric field levels. Fields in accelerators are still sometimes expressed in units of kilpatrick. Now, better physics models are known to predict the surface breakdown field, but kilpatrick is here to stay.

Input to CURLI, 2

The next step is to select the value of the radius parameter a . This is done by letting CURLI calculate a number of parameters for several different values of radius. We choose the option that the transverse and longitudinal space charge limit will be the same ($I_t = I_L$) at the end of the GB. Several lines are printed out for a series of values of a .

Based on many simulations, line 6 is selected, for the value of the aperture $a = 0.25$ cm.

Several other parameters are established here:

- $m = 1.756$, the modulation index
- $A = 0.461$, the acceleration parameter
- $r_0 = 0.351$ cm, the reference radius
- $V = 0.083$ MV, the vane-vane voltage
- $dW/dz = 4.01$ MV/m, the acceleration rate
- $\sigma_0 = 1.74$, the zero-current phase advance
- $D = -0.063$, the gap defocusing parameter
- $a_n = 0.174$ pi cm-mrad, the acceptance
- $\sigma_i/\sigma_0 = 0.678$, the fraction tune depression
- $kilp = 1.85$, the surface field in kilpatrick
- $cx = 0.109$ ampere, the maximum current

```
Enter Mass(amu),Q,IType(1=>RFQ,2=>pi-pi Wid,3=>pi-3pi Wid,4=>DTL
Phis(deg),current(mA) 1.0000 1.0000 1 -30.0000 70.0000
```

```
Psi,maximum (wg/wi)= 90.9 15.694
```

```
Enter Freq(MHz), Wi(MeV), Wfinal(MeV) 402.5000 .0650 2.5000
```

```
Enter Wgb(MeV) < 1.02 MeV, Esurface(kilpatrick) 0.75 1.85
.7500 MeV, 36.0183 MV/m, 1.8500 kilpatrick
```

```
Enter (1,a(cm),m,dm,nsteps) to find It,Il or (2,0,a,da,nsteps) to set It=Il
2 .0000 .2000 .0100 20.0000
```

```
*****
```

```
Beta= .04013 Wavel= 74.48 Beta*lambda= 2.989 Bz= .249
```

```
*****
```

n	a	m	A	r0	V	B	dwdz	sig0	del	ani/pi	si/s0	kilp	cx
1	.200	1.987	.556	.309	.075	4.670	1.891	26.1	.068	.115	.598	1.850	.091
2	.210	1.937	.537	.318	.077	4.515	1.870	25.0	.068	.127	.616	1.850	.095
3	.220	1.887	.517	.326	.078	4.377	1.841	24.0	.067	.139	.635	1.850	.099
4	.230	1.837	.497	.334	.080	4.254	1.803	23.2	.065	.151	.653	1.850	.102
5	.240	1.794	.478	.342	.081	4.132	1.769	22.4	.064	.163	.667	1.850	.106
6	.250	1.756	.461	.351	.083	4.010	1.740	21.5	.063	.174	.678	1.850	.109
7	.260	1.719	.443	.359	.085	3.899	1.705	20.7	.062	.185	.688	1.850	.112
8	.270	1.681	.425	.367	.086	3.798	1.664	20.1	.060	.198	.700	1.850	.115
9	.280	1.650	.409	.376	.088	3.694	1.630	19.3	.059	.208	.707	1.850	.118

```
*****
```

```
Enter line number of parameter choice to print out and exit, or 0 to repeat 6
```

```
*****
```

```
Beta= .04013 Wavel= 74.48 Beta*lambda= 2.989 Bz= .249
```

```
*****
```

n	a	m	A	r0	V	B	dwdz	sig0	del	ani/pi	si/s0	kilp	cx
1	.250	1.756	.461	.351	.083	4.010	1.740	21.5	.063	.174	.678	1.850	.109

```
*****
```

```
Enter I(mA) to track at , 6 x enorm(cm-mrad,n/pi (dist 6)) 60.000 .120
```

```
1.0000 1.0000 402.5000 .0650 .7500 2.5000 .0830
4.0104 .4606 -30.0000 -30.0000 60.0000 .1200 8 .4606
```

Input to CURLI, 3

After the parameters in the selection line 6 are printed out, the desired current to actually track, 60 mA is entered, along with the input beam emittance.

The input emittance to parmila may be confusing. **For historical reasons, the emittance is entered as six times the normalized emittance in units of cm-mr.**

However, in the actual input to PARMTEQ, the emittance is **six** times the unnormalized emittance in units of cm-radian. The input beam energy is 65 keV/n, so the normalized velocity $b = 0.0118$. Since the normalized emittance from the ion source is 0.02 p cm-mrad, the unnormalized emittance is 1.7 p cm-mrad = 0.0017 p cm-rad. Six times this is 0.01019, and will appear in the input file to the PARMTEQ code. This is the source of much confusion.

```
Enter Mass(amu),Q,IType(1=>RFQ,2=>pi-pi Wid,3=>pi-3pi Wid,4=>DTL
Phis(deg),current(mA) 1.0000 1.0000 1 -30.0000 70.0000
```

```
Psi,maximum (wg/wi)= 90.9 15.694
```

```
Enter Freq(MHz), Wi(MeV), Wfinal(MeV) 402.5000 .0650 2.5000
```

```
Enter Wgb(MeV) < 1.02 MeV, Esurface(kilpatrick) 0.75 1.85
```

```
.7500 MeV, 36.0183 MV/m, 1.8500 kilpatrick
```

```
Enter (1,a(cm),m,dm,nsteps) to find It,Il or (2,0,a,da,nsteps to set It=Il
```

```
2 .0000 .2000 .0100 20.0000
```

```
*****
```

```
Beta= .04013 Wavel= 74.48 Beta*lambda= 2.989 Bz= .249
```

```
*****
```

n	a	m	A	r0	V	B	dwdz	sig0	del	ani/pi	si/s0	kilp	cx
1	.200	1.987	.556	.309	.075	4.670	1.891	26.1	.068	.115	.598	1.850	.091
2	.210	1.937	.537	.318	.077	4.515	1.870	25.0	.068	.127	.616	1.850	.095
3	.220	1.887	.517	.326	.078	4.377	1.841	24.0	.067	.139	.635	1.850	.099
4	.230	1.837	.497	.334	.080	4.254	1.803	23.2	.065	.151	.653	1.850	.102
5	.240	1.794	.478	.342	.081	4.132	1.769	22.4	.064	.163	.667	1.850	.106
6	.250	1.756	.461	.351	.083	4.010	1.740	21.5	.063	.174	.678	1.850	.109
7	.260	1.719	.443	.359	.085	3.899	1.705	20.7	.062	.185	.688	1.850	.112
8	.270	1.681	.425	.367	.086	3.798	1.664	20.1	.060	.198	.700	1.850	.115
9	.280	1.650	.409	.376	.088	3.694	1.630	19.3	.059	.208	.707	1.850	.118

```
*****
```

```
Enter line number of parameter choice to print out and exit, or 0 to repeat 6
```

```
*****
```

```
Beta= .04013 Wavel= 74.48 Beta*lambda= 2.989 Bz= .249
```

```
*****
```

n	a	m	A	r0	V	B	dwdz	sig0	del	ani/pi	si/s0	kilp	cx
1	.250	1.756	.461	.351	.083	4.010	1.740	21.5	.063	.174	.678	1.850	.109

```
*****
```

```
Enter I(mA) to track at , 6 x enorm(cm-mrad,n/pi (dist 6)) 60.000 .120
```

```
1.0000 1.0000 402.5000 .0650 .7500 2.5000 .0830
4.0104 .4606 -30.0000 -30.0000 60.0000 .1200 8 .4606
```

Input to RFQUIK

The RFQUIK code generates a table that is used by PARMTEQ to generate each cell in the RFQ. The RFQUIK output table lists the parameters at a few values of z along the RFQ, and PARMTEQ interpolates these values for the detailed cell table.

RFQUIK needs a few more parameters. The first two lines are input automatically from CURLI. The third input line is first used to generate a set of values for a range of W_s , the energy at the end of the shaper section (SH). Here, only one energy is input, the value having been previously determined by many simulations. $W_s = 0.070$ MeV.

The output file, here called tape1.dat, is the input file for PARMTEQ and contains additional information about the matched beam Twiss parameters calculated for the ion current requested and some additional PARMTEQ input data.

Enter q,mass(amu),freq(MHz),Wi(MeV),Wg(MeV),Wf(MeV),V(MV)

1.0 1.0000 402.5 .0650 .750 2.500 .0830

Enter B,Aag,phig(deg),phif(deg),I(mA),En(cm-mr),ncrm,Aend

4.0104 .461 -30.00 -30.00 60.0 .120 8 .461

Enter lshaper(1 OR 2),lambda,reff(cm),Ws(MeV) > .065, dex(MeV),nsteps (-1 to quit)

1 .00000 .00000 .07000 .00000 0

Ws Capture Pack Sigmamin Power(kW) L(cm) EL(MeV-sec) ELn(cm-mr)
.070 1.00 .24 11.9 759.0 376. .141E-11 .452E-01

Lr,Ls,Lg,La,Lt= 3.5 54.1 172.3 146.1 376.1 cm
dsc,drfnl,2l1/ka,sigma = -.07 -.09 1.42 11.9
Pcu,Pb,Pt(kW)= 612.9 146.1 759.0

z	B	phi	m	V	W	A	a	psi
-3.520	.201	-90.000	1.000	.083	.065	.000	1.570	360.000
.000	4.010	-90.000	1.000	.083	.065	.000	.351	360.000
13.524	4.010	-88.733	1.018	.083	.065	.005	.348	329.497
27.048	4.010	-87.466	1.036	.083	.066	.011	.345	316.479
40.572	4.010	-86.200	1.053	.083	.067	.016	.342	306.255
54.096	4.010	-84.933	1.069	.083	.070	.022	.340	297.451
126.822	4.010	-70.671	1.083	.083	.119	.039	.337	228.546
151.784	4.010	-61.073	1.106	.083	.167	.059	.334	192.495
166.979	4.010	-54.441	1.133	.083	.216	.081	.330	169.443
177.922	4.010	-49.554	1.165	.083	.264	.107	.325	153.083
186.477	4.010	-45.772	1.200	.083	.313	.134	.319	140.699
193.502	4.010	-42.735	1.239	.083	.361	.164	.314	130.904
199.463	4.010	-40.230	1.283	.083	.410	.195	.307	122.906
204.640	4.010	-38.118	1.331	.083	.459	.228	.301	116.215
209.215	4.010	-36.305	1.384	.083	.507	.263	.293	110.509
213.315	4.010	-34.729	1.443	.083	.556	.300	.286	105.569
217.028	4.010	-33.341	1.508	.083	.604	.338	.278	101.238
220.421	4.010	-32.107	1.581	.083	.653	.377	.269	97.399
223.546	4.010	-31.000	1.663	.083	.701	.418	.260	93.966
226.441	4.010	-30.000	1.756	.083	.750	.461	.250	90.873
372.587	4.010	-30.000	1.677	.083	2.500	.461	.255	90.873

Input File to PARMTEQ

The input file, **tape1.dat**, contains the output of RFQUIK, along with additional information needed, such as the beam parameters, some parameters controlling the output data and the space charge parameters. This file may be edited to further improve the performance of the RFQ.

PARMTEQ will generate a beam bunch with the proper Twiss parameters and track it through the RFQ. The values of each macroparticle for each cell are written to a large file for subsequent analysis, such as plotting a phase space diagram for each cell in the RFQ.

```
run 1 1
title
  Design ,Freq=402.50 Mhz, q=1.0,Wi= .065,Wf= 2.50 amu= 1.00 I=
60.0mA
linac 1 .065 402.50 1
tank 1 2.500 0 0 0 0 0 0 0 0 8 0 0 0 0 0 0 0 0 0 0 0 0
zdata -5 -3.520 .201 -90.000 1.000 .0830
      0.0 4.010 -90.000 1.000 .0830 8
zdata -5 .000 4.010 -90.000 1.000 .0830
      13.524 4.010 -88.733 1.018 .0830
      27.048 4.010 -87.466 1.036 .0830
      40.572 4.010 -86.200 1.053 .0830
      54.096 4.010 -84.933 1.069 .0830
      126.822 4.010 -70.671 1.083 .0830
      151.784 4.010 -61.073 1.106 .0830
      166.979 4.010 -54.441 1.133 .0830
      177.922 4.010 -49.554 1.165 .0830
      186.477 4.010 -45.772 1.200 .0830
      193.502 4.010 -42.735 1.239 .0830
      199.463 4.010 -40.230 1.283 .0830
      204.640 4.010 -38.118 1.331 .0830
      209.215 4.010 -36.305 1.384 .0830
      213.315 4.010 -34.729 1.443 .0830
      217.028 4.010 -33.341 1.508 .0830
      220.421 4.010 -32.107 1.581 .0830
      223.546 4.010 -31.000 1.663 .0830
      226.441 4.010 -30.000 1.756 .0830
      372.587 4.010 -30.000 1.677 .0830 -1
rfqout 1
start 1
stop -1
elimit .0943
homode 1 1 1 1 1 1 1 1
input 6 2000 1.66 6.82 .010158 1.66 6.82 .010158 180.0
output 3 1 0 0 0 1 1
output 2 1 0 0 0 1 1 2000 1
output 4 1 0 0 0 1 1
scheff 60.0 .0351 .0440 10 20 5 10
begin
end
```

PARMTEQ Output

Here is a sample of a small part of the PARMTEQ output. The cell table is first printed out, and then the transmission and loss fraction for each cell in the RFQ.

The RFQ is 372.27 cm long and contains 449 cells.

Here, 94.4% of the 60 mA beam from the ion source was accelerated to full energy, 4.4% was lost on the vane tips and 1.1% lost from the longitudinal bucket.

The actual RFQ beam current is specified at 38 mA, so the RFQ is capable of higher current for future upgrades of the SNS facility.

Tank 1 Length = 372.27 cm, 449 Cells

```

Nc V   Ws 1E3beta Ez  CapA phi  a  m  B  rfd Lc Ltot ltransv llong chi Ea/Es
0 83.0 65.00 11.77 .000 .000 -90.0 .852 1.000 .00 .00 .438 .44 .00 .00 1.000 .000
1 83.0 65.00 11.77 .000 .000 -90.0 .852 1.000 .68 .00 .438 .88 1797.06 .00 1.000 .000
2 83.0 65.00 11.77 .000 .000 -90.0 .550 1.000 1.15 .00 .438 1.32 436.95 .00 1.000 .000
3 83.0 65.00 11.77 .000 .000 -90.0 .484 1.000 2.10 .00 .438 1.75 360.00 .00 1.000 .000
4 83.0 65.00 11.77 .000 .000 -90.0 .437 1.000 2.57 .00 .438 2.19 345.18 .00 1.000 .000
5 83.0 65.00 11.77 .000 .000 -90.0 .401 1.000 3.05 .00 .438 2.63 346.46 .00 1.000 .000
6 83.0 65.00 11.77 .000 .000 -90.0 .373 1.000 3.52 .00 .438 3.07 353.64 .00 1.000 .000
7 83.0 65.00 11.77 .000 .000 -90.0 .350 1.000 4.00 .00 .438 3.51 363.21 .00 1.000 .000
8 83.0 65.00 11.77 .003 .000 -90.0 .350 1.001 4.01 .00 .438 3.95 362.24 1.04 .999 .000
9 83.0 65.00 11.77 .007 .000 -89.9 .350 1.001 4.01 .00 .438 4.38 360.93 2.11 .999 .000
444 83.0 2376.19 71.03 1.460 .464 -30.0 .254 1.686 4.01 -.02 2.637 358.87 218.05 113.59 .526 .033
445 83.0 2402.39 71.42 1.451 .463 -30.0 .254 1.685 4.01 -.02 2.651 361.52 219.56 113.53 .526 .033
446 83.0 2428.57 71.81 1.441 .463 -30.0 .254 1.683 4.01 -.02 2.666 364.19 221.07 113.48 .527 .033
447 83.0 2454.72 72.19 1.432 .462 -30.0 .254 1.682 4.01 -.02 2.680 366.87 222.57 113.42 .527 .033
448 83.0 2480.84 72.58 1.423 .462 -30.0 .254 1.681 4.01 -.02 2.694 369.56 224.07 113.37 .528 .032
449 83.0 2506.93 72.95 1.414 .461 -30.0 .254 1.679 4.01 -.02 2.709 372.27 225.57 113.31 .529 .032
Nc V   Ws 1E3beta Ez  CapA phi  a  m  B  rfd Lc Ltot ltransv llong chi Ea/Es
start 1
stop -1
elimit .0943
homode 1 1 1 1 1 1 1 1
input 6 2000 1.66 6.82 .010158 1.66 6.82 .010158 180.0
output 3 1 0 0 0 1 1
output 2 1 0 0 0 1 1 2000 1
output 4 1 0 0 0 1 1
scheff 60.0 .0351 .0440 10 20 5 10
begin
  2 100.0% .0% .0 .88
  3 100.0% .0% .0 1.32
  4 100.0% .0% .0 1.75
  5 100.0% .0% .0 2.19
  6 100.0% .0% .0 2.63
  7 100.0% .0% .0 3.07
  8 100.0% .0% .0 3.51
  9 100.0% .0% .0 3.95
 10 100.0% .0% .0 4.38
ncell %good %badT %badL, z 2000 particles
444 94.4% 4.4% 1.1 358.87
445 94.4% 4.4% 1.1 361.52
446 94.4% 4.4% 1.1 364.19
447 94.4% 4.4% 1.1 366.87
448 94.4% 4.4% 1.1 369.56
449 94.4% 4.4% 1.1 372.27
END OF RUN 1

```

Appendix

More rigorous treatment of RFQ beam dynamics

Electric Alternating Gradient Focusing

The electrodes generate an electric quadrupole field. The potentials on the electrodes are

$$V = \pm \frac{1}{2} V_0 \cos \omega t$$

For a radius of the pole tip of a , the fields are

$$E_x = g_0 x, \quad E_y = -g_0 y, \quad g_0 = \frac{V_0}{a^2}$$

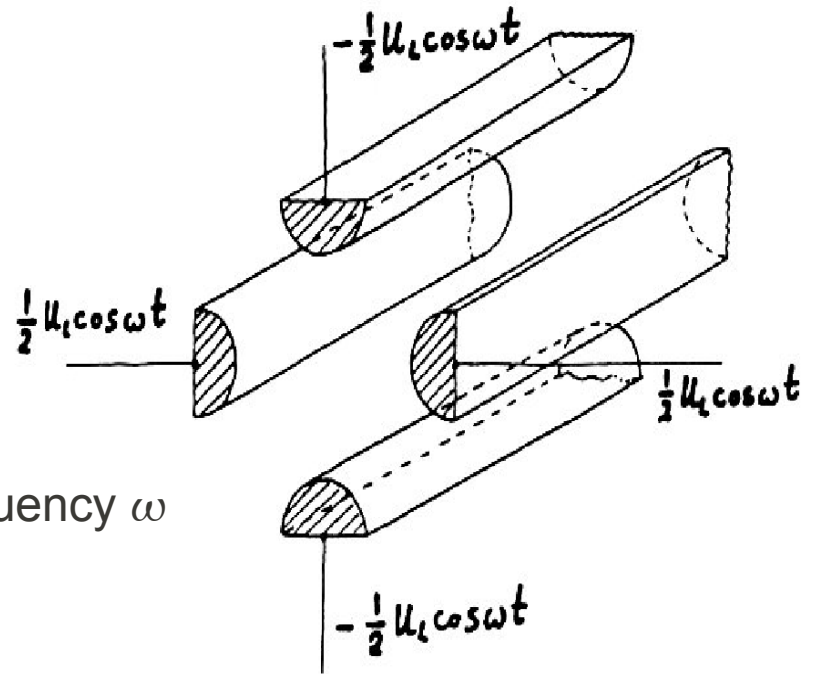
For a sinusoidal variation of the voltage at frequency ω the equation of transverse motion is

$$m \ddot{x} = qe E_x = qe g_0 \sin(\omega t) x$$

The time-varying voltage polarity gives rise to an alternating-gradient focusing, just as in a series of fixed quadrupoles of alternating polarity.

Using nomenclature common to RFQ design formulas, $\beta^2 \lambda^2 \frac{d^2 x}{dz^2} = B_0 \sin(kz) x$

where $k = \frac{2\pi}{\beta \lambda}$ and we define the unitless focusing parameter $B_0 = \chi \left(\frac{qeV}{mc^2} \right) \frac{\lambda^2}{a^2}$



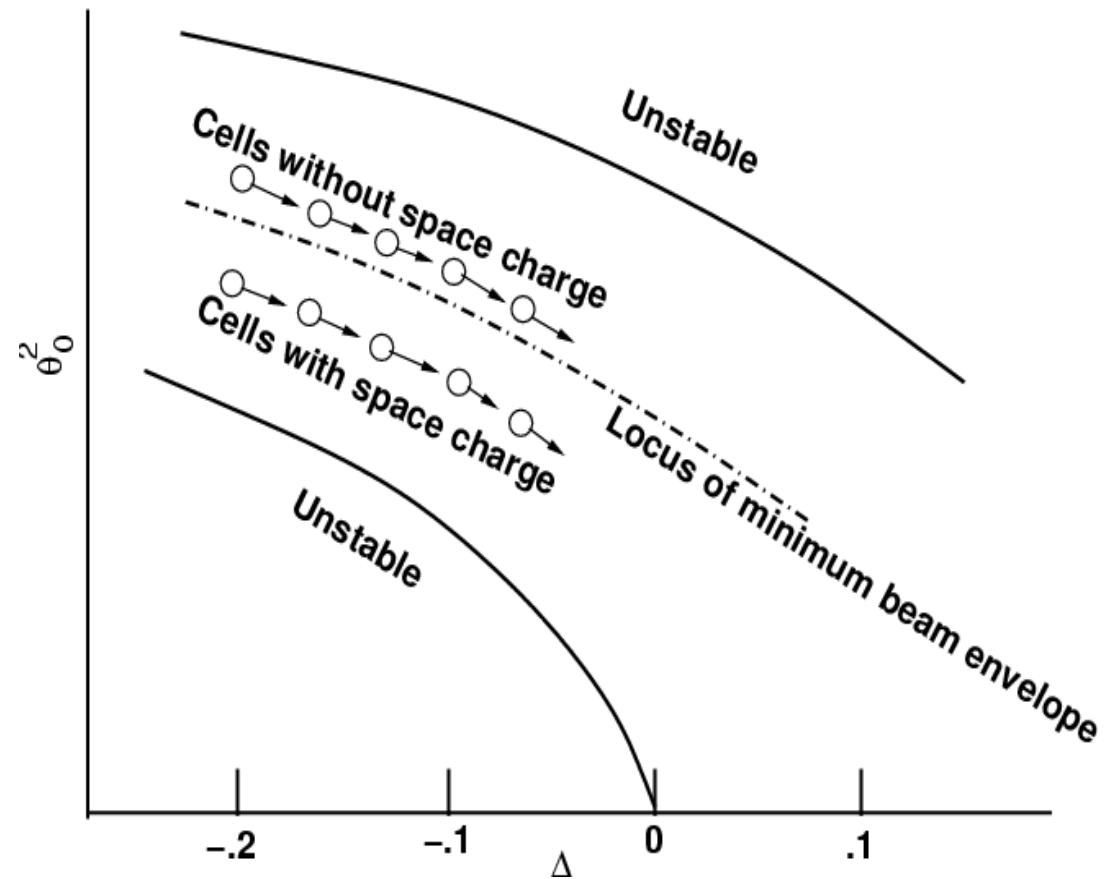
Focusing Stability Plot for RFQ

As with Drift-Tube linacs, an RFQ stability plot indicates the region of beam stability as a function of the focusing strength $B = \theta^2$ and the gap defocusing term Δ_{gap} .

$$B_0 \equiv \theta_0^2 = \chi \left(\frac{qeV}{mc^2} \right) \frac{\lambda^2}{a^2}$$

In the case of the RFQ, the gap defocusing term

$$\Delta_{\text{gap}} = \frac{\pi^2}{2} \left(\frac{qeV}{mc^2} \right) \frac{A}{\beta^2} \sin \phi_s$$



scales as $1/\text{Energy}$ and therefore is significant at the low energy end of the RFQ.

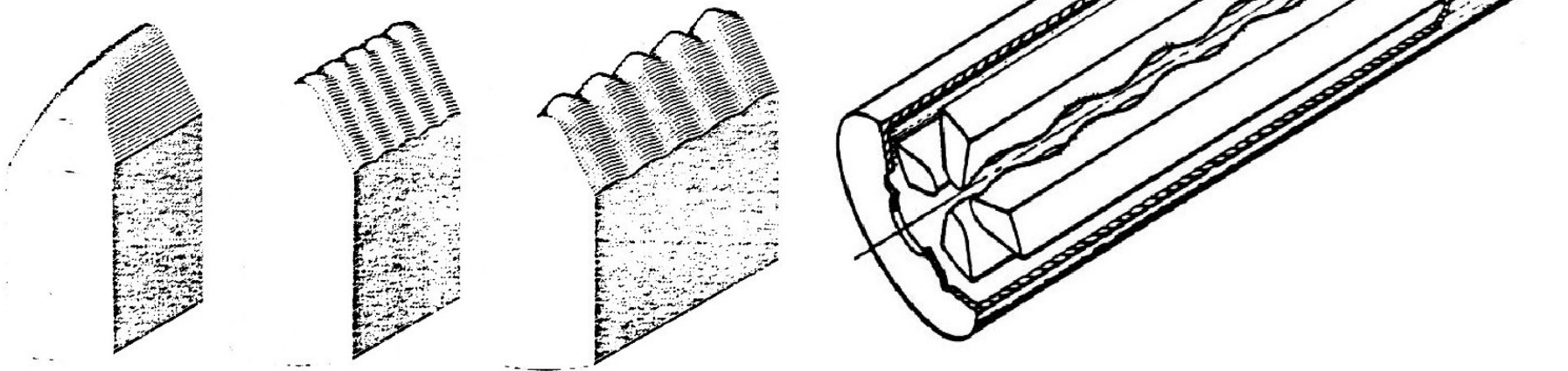
For an RFQ with uniform vane voltage V along its length (the usual case) the transverse focusing strength is nearly constant, varying with c and with a , which have relatively narrow ranges.

Generating Longitudinal Accelerating Field

The four vanes, excited with a TE_{210} field, generate a transverse quadrupole field. If the vanes are smooth, no longitudinal field is produced.

If the vanes are modulated, and the phase of the modulation on the even tips and the odd tips is opposite (even close when odd far away), a longitudinal field component E_z is generated. The amplitude of E_z is controlled by the depth of the modulation of the vane tip. The modulations are approximately sinusoidal, and are the solution of an implicit equations that must be solved numerically.

A **unit cell** comprises one-half of an oscillation of the vane tip, and is $bl/2$ long. The RFQ comprises N unit cells in its design.



Potential Expansion

The potential on the axis is expanded in a Fourier-Bessel infinite series

$$U(r, \theta, z) = \frac{V}{2} \left[\sum_{m=1}^{\infty} A_{0m} \left(\frac{r}{r_0} \right)^{2m} \cos(2m\theta) + \sum_{m=0}^{\infty} \sum_{n=1}^{\infty} A_{nm} I_{2m}(nkr) \cos(2m\theta) \cos(nkz) \right]$$

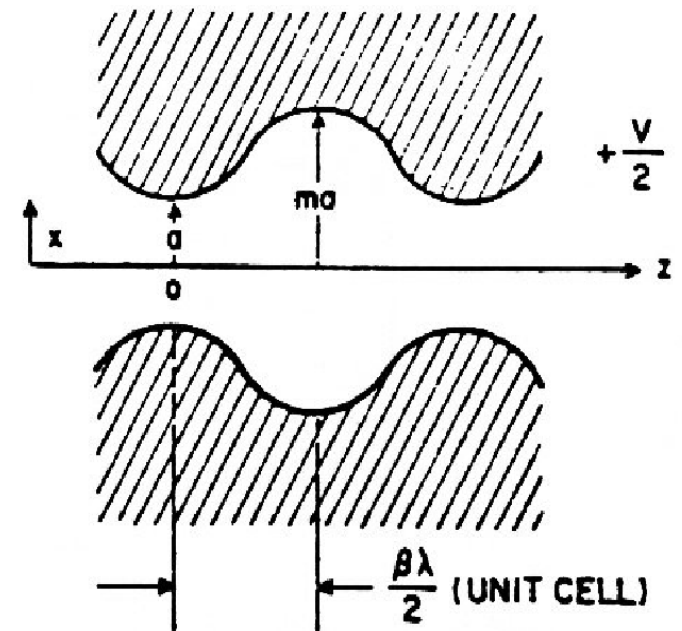
The coefficients A_{nm} are chosen so the potential U is matched at the pole tip surfaces.

Selecting the **two leading terms** of each summation, adequate as a first approximation,

$$U_{two-term}(r, \theta, z) = \frac{V}{2} \left[\left(\frac{r}{r_0} \right)^2 \cos(2\theta) + A I_0(kr) \cos(kz) \right]$$

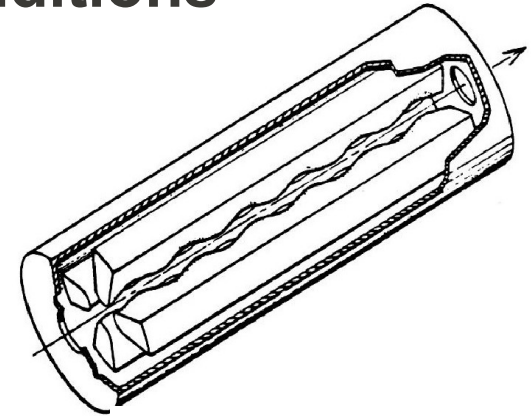
The first term represents the quadrupole nature of the potential, and the second term will generate the longitudinal field as a function of the parameter $A = A_{10}$, the **acceleration parameter**, which is linked to the geometry of the modulations of the vane tip.

The parameter m is the **modulation parameter**, describing the depth of the modulation.



Satisfying the Boundary Conditions

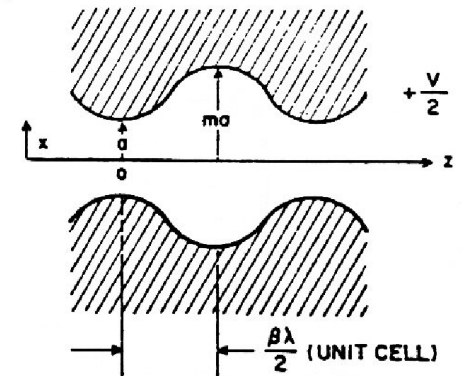
The potential at the surface of the pole is $+V/2$ or $-V/2$.
When, say, the even vanes are distance a from the axis,
the odd vanes are a distance ma from the axis.



The potential function $U(r, \theta, z)$ becomes, at $z=0$,

$$U(a, 0, 0) = U(ma, 0, L_c) = \frac{V}{2}$$

$$U(ma, \frac{\pi}{2}, 0) = U(m, \frac{\pi}{2}, L_c) = -\frac{V}{2}$$



The two-term potential function then gives

$$\left(\frac{a}{r_0}\right)^2 + AI_0(ka) = 1, \quad \left(\frac{ma}{r_0}\right)^2 - AI_0(mka) = 1, \quad k = \frac{\pi}{L_c} = \frac{2\pi}{\beta\lambda}$$

Solve for the acceleration parameter A is given by the geometry of the cell and r_0 :

$$A = \frac{m^2 - 1}{m^2 I_0(ka) + I_0(mka)}$$

m , the modulation index, is a number equal or greater than 1. If $m = 1$, $A = 0$, and there is no modulation of the vane tip and no longitudinal field.

The Normalizing Radius r_0

Solving the boundary condition also gives r_0 , the normalizing radius:

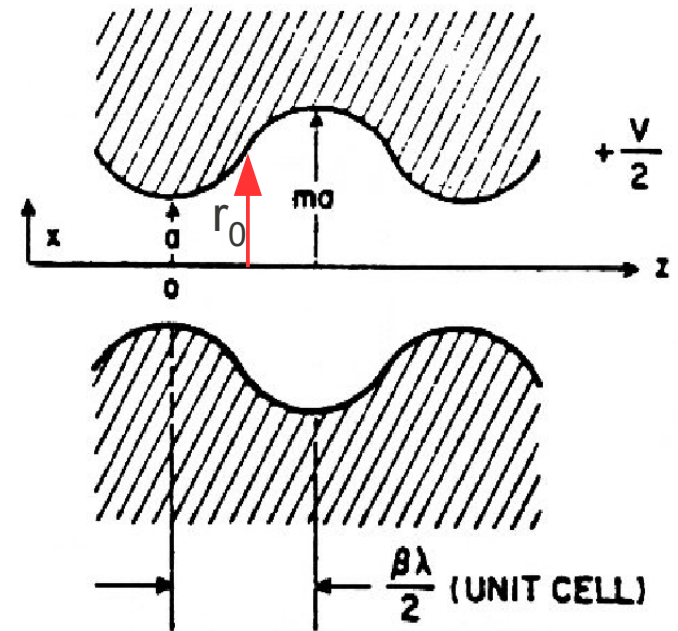
$$\left(\frac{a}{r_0}\right)^2 = 1 - A I_0(ka)$$

$$A = \frac{m^2 - 1}{m^2 I_0(ka) + I_0(mka)}$$

r_0 is the radius in the middle of the cell where the the distance from the axis to the pole tips is identical for both the even and odd poles.

At one end of the cell, the radii are a and ma , for the even and the odd vane tips, and at the other end the radii are ma and a .

At one point in the cell, in the middle, the two radii are equal and are r_0 .



The Focusing Efficiency Parameter χ

$$\left(\frac{a}{r_0}\right)^2 = 1 - AI_0(ka), \quad r_0 = \frac{a}{\sqrt{1 - AI_0(ka)}}$$

We define the focusing efficiency parameter χ as

$$\chi \equiv 1 - AI_0(ka)$$

so

$$r_0 = \frac{a}{\sqrt{\chi}}, \quad a \leq r_0 \leq ma$$

We will see that χ modifies the transverse focusing effectiveness. χ is a number 1 or less. As the modulation increases, the modulations in the vane tip reduce the strength of the transverse focusing strength.

χ is a value dependent only on the geometry of the vane tip profile, as is A , the acceleration parameter.

The Fields

The fields are found as the derivative of the potential in cylindrical coordinates.

$$E_r = -\frac{\chi V}{a^2} r \cos(2\theta) - \frac{kAV}{2} I_1(kr) \cos(kz),$$

$$E_\theta = \frac{\chi V}{a^2} r \sin(2\theta),$$

$$E_z = \frac{kAV}{2} I_0(kr) \sin(kz)$$

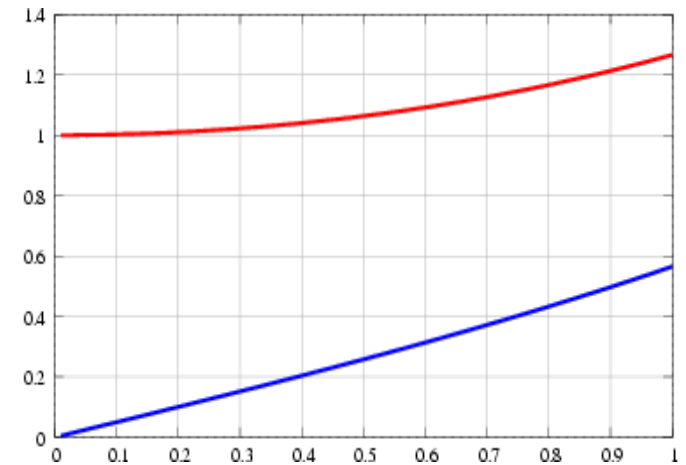
The $\frac{\chi V}{a^2} r \begin{Bmatrix} \cos(2\theta) \\ \sin(2\theta) \end{Bmatrix}$ terms are the transverse electrostatic quadrupole field.

The focusing efficiency parameter c , which depends on the modulation depth, is the reduction in transverse focusing field as the modulation depth increases.

The term in E_z is the longitudinal acceleration field and increases slightly at the pole tip.

The $\frac{kAV}{2} I_1(kr) \cos(kz)$ term is the transverse

defocusing term, which is proportional to the accelerating field strength and increases approximately with radius.



$I_0(x)$ and $I_1(x)$

Energy Gain in a Unit Cell

The acceleration parameter A is a function of the modulation depth m

$$A = \frac{m^2 - 1}{m^2 I_0(ka) + I_0(mka)}$$

The longitudinal field is

$$E_z = \frac{kAV}{2} I_0(kr) \sin(kz) = \frac{kAV}{2} \sin(kz) \text{ on axis.} \quad k = \frac{2\pi}{\beta\lambda} = \frac{\pi}{L_c}$$

The voltage integral across the $L_c = \frac{\beta\lambda}{2}$ cell is then $\Delta V_c = \int_0^{L_c} E_z dz = AV$

The accelerating voltage across the cell is the vane-vane voltage V times A .

An ion traveling along the axis with phase ϕ_s relative to the RF phase will pick up a lesser energy, taking into account both the phase of the ion with respect to the RF phase, and the **transit time factor** for the field profile in the cell, which is $\pi/4$ for the field profile for the RFQ cell.

$$\Delta W = qe \int_0^{L_c} E_z \sin(kz) dz = \frac{\pi}{4} AV \cos \phi_s$$

RF Defocusing in the RFQ Gap

Recall that the radial component of the field in the gap gives the ion a radial kick. For the drift-tube accelerator, a unitless defocusing parameter was defined:

$$\Delta_{gap,RFQ} = \frac{\pi^2}{2} \frac{q e V}{m c^2} \frac{A}{\beta^2} \sin \phi_s$$

which produces a radial kick r' , proportional to the radial displacement r :

$$\Delta_{gap} = -\frac{\Delta r'}{r} L_{cell} = -\frac{\Delta r'}{r} \beta \lambda$$

For an RFQ,

$$\Delta_{gap,RFQ} = \frac{\pi^2}{2} \frac{q e V}{m c^2} \frac{A}{\beta^2} \sin \phi_s$$

So the (unitless) gap defocusing term for the RFQ is

$$\Delta_{gap} = -\frac{\Delta r'}{r} L_{cell} = -\frac{\Delta r'}{r} \beta \lambda$$

Peak Surface Field on Vanetips

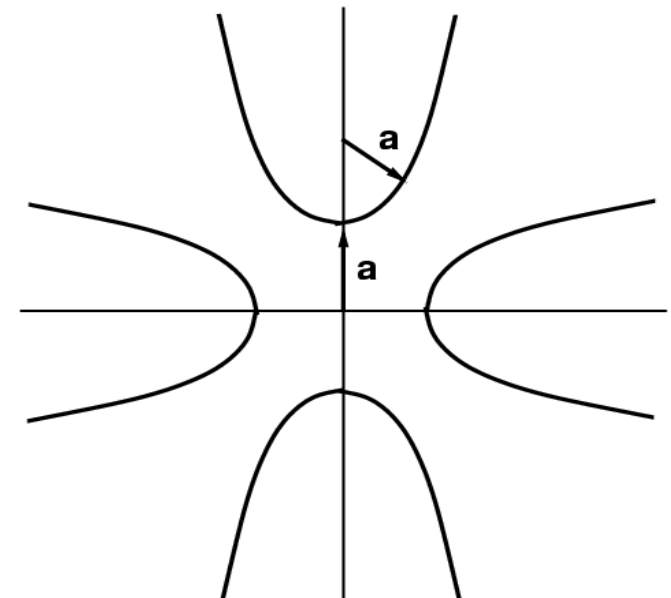
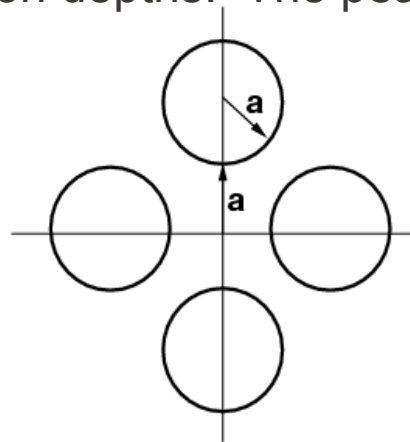
A sensitive parameter to RFQ performance is the peak field that can be sustained between the vane tips. The ability to focus and accelerate the beam improves with higher vane tip voltage. The limit is constrained by the tendency for the vane tips to exhibit spark breakdown.

The geometry of the vane tips effects the peak surface field. In the approximation of cylinder vanetip profiles with radius a , and the nearest approach of the vanetip to the axis is also a , the peak field between the vanetips is $1.25 V/a$, with the potential of the vanetips $+V/2$ and $-V/2$.

The ideal profile of a vanetip is hyperbolic, and the peak field for unmodulated vanes is $1.38 V/a$. When the vane is modulated ($m > 1$), the peak field is increased.

A field enhancement factor k is defined and tabulated for various vanetip shapes and modulation depths. The peak vanetip field is

$$E_{surface} = \frac{\kappa V}{r_0}$$



Bravery Factor

The selection of the peak vanetip field (bravery factor) has a strong influence on the performance of the RFQ.

High peak fields increase the RFQ performance in areas of:

- Higher acceptance (for larger emittance beams)
- Greater space charge capability
- Accept heavy ions with lower charge state
- Shorter RFQ

but also have the effect of:

- Increased probability of sparking
- More RF power required over a lower-gradient design

The kilpatrick criterion for sparking as a function of frequency is (E in MV/m)

$$f [MHz] = 1.64 E^2 e^{\frac{-8.5}{E}}$$

For the highest reliability, the peak surface field E_{surface} is held to below 2 kilpatrick and even less for RFQs that operate CW, rather than pulsed. Very brave designs have been made up to 2.4 kilpatrick or so, with a lot of sparking to be expected.

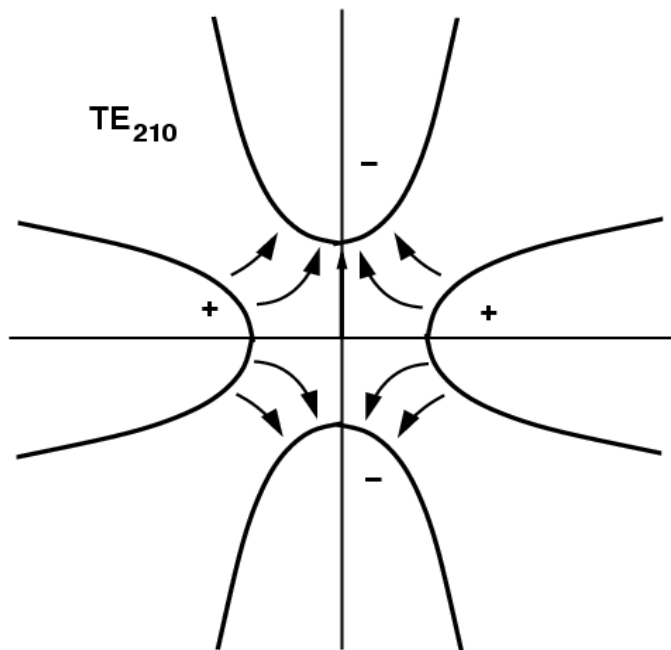
The TE_{210} and TE_{110} Modes of an RFQ

TE_{210} (quadrupole) mode.

$E_y = 0$ along the x-axis

$E_x = 0$ along the y axis

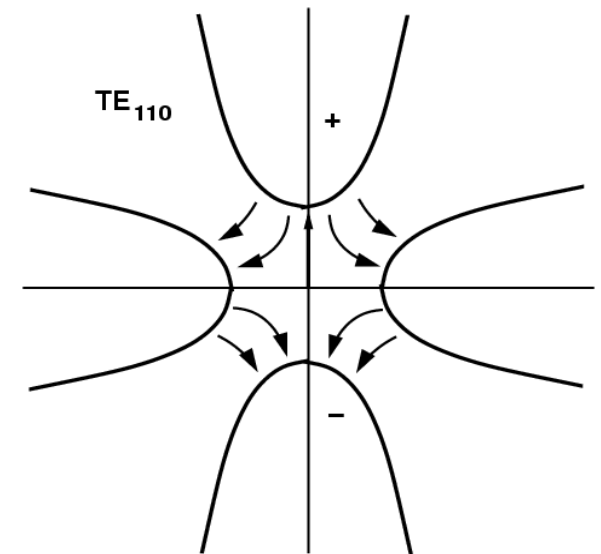
A vacuum boundary exists from the origin to each of the vane tips.



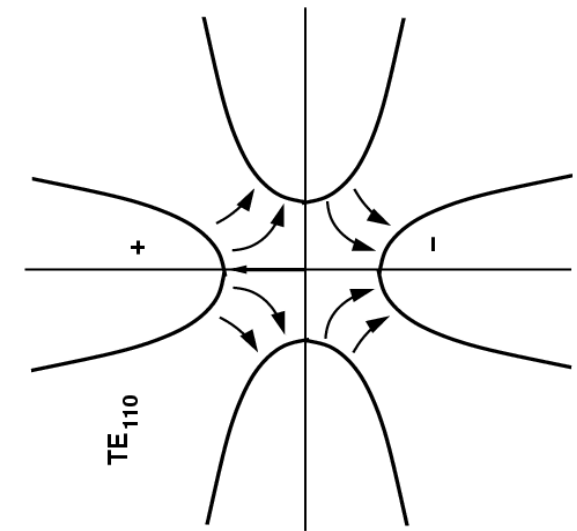
The two TE_{110} modes.

They are usually nearly degenerate in frequency.

In the upper figure, the electric field is perpendicular to the x-axis and the y-axis is a symmetry plane.



In designing an RFQ, the TE_{210} and TE_{110} mode frequencies are calculated, and their separation is a measure of the field stability of the structure. It is possible to have a degeneracy of the TE_{210} and TE_{110} frequencies.



Spatial and Temporal Variation

It is important to understand the difference between the spatial variation of the vane tip modulation and the temporal variation of the field which produces the strong focusing period.

The spatial variation of the vane tips generates the accelerating cells. The length of each cell is $\beta\lambda/2$, and is incorporated into the geometry of the structure. The strength of the longitudinal field E_z is governed by the depth of the modulation. As the beam accelerates, each cell grows longer as β is increasing.

The transverse focusing period is $\beta\lambda$, and is present even if there is no modulation of the vane tips.